

NACA TN 2181 9093



# NATIONAL ADVISORY COMMITTEE FOR AERONAUTICS

TECHNICAL NOTE 2181

THE AERODYNAMIC FORCES AND MOMENTS ON A  $\frac{1}{10}$ -SCALE MODEL  
OF A FIGHTER AIRPLANE IN SPINNING ATTITUDES AS  
MEASURED ON A ROTARY BALANCE IN THE Langley  
20-FOOT FREE-SPINNING TUNNEL

By Ralph W. Stone, Jr., Sanger M. Burk, Jr.,  
and William Bihrlle, Jr.

Langley Aeronautical Laboratory  
Langley Air Force Base, Va.



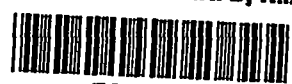
Washington

September 1950

TECHNICAL NOTE 2181

15-11-1

15-11-1



0065137

## NATIONAL ADVISORY COMMITTEE FOR AERONAUTICS

## TECHNICAL NOTE 2181

THE AERODYNAMIC FORCES AND MOMENTS ON A  $\frac{1}{10}$ -SCALE MODEL  
OF A FIGHTER AIRPLANE IN SPINNING ATTITUDES AS  
MEASURED ON A ROTARY BALANCE IN THE LANGLEY  
20-FOOT FREE-SPINNING TUNNEL

By Ralph W. Stone, Jr., Sanger M. Burk, Jr.,  
and William Bahrle, Jr.

## SUMMARY

An investigation was conducted to provide general information on the magnitudes and directions of the aerodynamic forces and moments exerted on a model of a fighter airplane in spinning attitudes as measured on a rotary balance installed in the Langley 20-foot free-spinning tunnel. The investigation included the determination of the effect on the aerodynamic forces and moments of reversing the rudder, of modifying the tail, and of deflecting the flaps and lowering the landing gear. The  $\frac{1}{10}$ -scale model was mounted on the rotary balance at attitudes simulating spinning conditions of a previously tested  $\frac{1}{20}$ -scale dynamic model and at other arbitrary spinning attitudes.

The results indicated that the primary effect of rudder reversal was to give a relatively large increment of anti-spin yawing-moment coefficient when compared with the magnitude of the aerodynamic yawing-moment coefficient of the fully developed spin; the other force and moment coefficients were affected to a much less degree. The increment of yawing-moment coefficient due to rudder reversal increased with decreasing angle of attack. Moving the horizontal tail rearward for this design increased the rudder-reversal effectiveness; deflecting the landing flaps reduced the rudder-reversal effectiveness. A conservative estimate from the experimental results indicates that a total aerodynamic yawing-moment coefficient ranging from approximately 0.021 to 0.025, against the spin, may be required for satisfactory recoveries from steep spins. Larger values of yawing-moment coefficient may be required for flatter spins. The aerodynamic force and moment measurements were in qualitative agreement with free-spinning results as regards spin and recovery characteristics.

## INTRODUCTION

The spinning and the spin recovery of airplanes have always been subjects of concern to manufacturers and pilots. It was realized in the past that the effects of the various components of an airplane on the spin and spin recovery could be determined by measurements of the aerodynamic forces and moments exerted on the spinning airplane. Measurements were made, therefore, of the aerodynamic characteristics of small models of rotating wings and airplanes by the use of an intricate spinning balance in the former N.A.C.A. 5-foot vertical wind tunnel. The results of these investigations are presented in references 1 to 9. With the advent of the Langley 15-foot free-spinning tunnel (reference 10), however, use of spin-balance measurements for estimating possible spin and recovery characteristics of airplanes was discontinued in favor of the visually observed and recorded spin and recovery characteristics of free-spinning models. The results of free-spinning investigations have led to empirical criterions (references 11 to 13), based on general geometric and mass characteristics of numerous designs investigated, from which airplanes may be designed with reasonable assurance that they will have satisfactory spin-recovery characteristics.

In order to augment the results of free-spinning tests, to obtain a broader understanding of the spin and spin recovery, and also to improve existing criterions, measurements of the aerodynamic forces and moments of spinning models of fighters were believed to be desirable. The existing information about these aerodynamic characteristics (references 1 to 9) was not considered sufficiently extensive for or applicable to airplanes of current design, and therefore a new and simpler rotary balance was devised and installed in the Langley 20-foot free-spinning tunnel.

For the present investigation, a  $\frac{1}{10}$ -scale model of a fighter airplane, suitable for testing on the rotary balance, was constructed. The free-spinning results of a  $\frac{1}{20}$ -scale dynamic model of this airplane were available from a previous investigation. The  $\frac{1}{10}$ -scale model was used to measure the force and moment coefficients acting on the airplane for the spins previously obtained with the free-spinning  $\frac{1}{20}$ -scale model.

This investigation provides general information on the magnitudes and directions of the aerodynamic forces and moments acting on a fighter airplane in fully developed spins. The investigation includes the determination of the effects on the aerodynamic forces and moments of varied rudder setting with and against the spin, of tail modifications, and of deflected flaps and lowered landing gear.

## SYMBOLS

The forces and moments were measured with respect to the body axes. A diagram of these axes showing the positive directions of the forces and moments is presented in figure 1.

$C_x$	longitudinal-force coefficient	$(X / \frac{1}{2} \rho V^2 S)$
$C_y$	lateral-force coefficient	$(Y / \frac{1}{2} \rho V^2 S)$
$C_z$	normal-force coefficient	$(Z / \frac{1}{2} \rho V^2 S)$
$C_R$	resultant-force coefficient	
$C_l$	rolling-moment coefficient	$(L / \frac{1}{2} \rho V^2 b S)$
$C_m$	pitching-moment coefficient based on wing span	$(M / \frac{1}{2} \rho V^2 b S)$
$C_n$	yawing-moment coefficient	$(N / \frac{1}{2} \rho V^2 b S)$
X	longitudinal force acting along X body axis, positive forward, pounds	
Y	lateral force acting along Y body axis, positive to right, pounds	
Z	normal force acting along Z body axis, positive downward, pounds	
L	rolling moment acting about X body axis, positive when it tends to lower right wing, foot-pounds	
M	pitching moment acting about Y body axis, positive when it tends to increase the angle of attack, foot-pounds	
N	yawing moment acting about Z body axis, positive when it tends to turn airplane to right, foot-pounds	
p	rolling angular velocity about X body axis, radians per second	
q	pitching angular velocity about Y body axis, radians per second	

r	yawing angular velocity about Z body axis, radians per second
$\frac{dp}{dt}$	rate of change of rolling angular velocity with time
$\frac{dq}{dt}$	rate of change of pitching angular velocity with time
$\frac{dr}{dt}$	rate of change of yawing angular velocity with time
$\Omega$	full-scale angular velocity about spin axis, radians per second unless otherwise indicated
$\Omega_b/2V$	spin coefficient .
S	wing area, square feet
b	wing span, feet
$\rho$	air density, slugs per cubic foot
V	free-stream velocity in balance tests, or full-scale true rate of descent in free-spinning tests, feet per second
$\bar{c}$	mean aerodynamic chord, feet
c	local chord, feet
$R_s$	spin radius, distance from spin axis to center of gravity, feet
$x/\bar{c}$	ratio of distance of center of gravity rearward of leading edge of mean aerodynamic chord to mean aerodynamic chord
$z/\bar{c}$	ratio of distance between center of gravity and thrust line to mean aerodynamic chord (positive when center of gravity is below thrust line)
W	weight of airplane, pounds
g	acceleration due to gravity, 32.2 feet per second per second
m	mass of airplane, slugs ( $W/g$ )
$\mu$	airplane relative-density coefficient ( $m/\rho Sb$ )

$I_x, I_y, I_z$	moments of inertia about X, Y, and Z body axes, respectively, slug-feet <sup>2</sup>
$\frac{I_x - I_y}{mb^2}$	inertia yawing-moment parameter
$\frac{I_y - I_z}{mb^2}$	inertia rolling-moment parameter
$\frac{I_z - I_x}{mb^2}$	inertia pitching-moment parameter
$\alpha$	angle between vertical and X body axis (approx. equal to absolute value of angle of attack at plane of symmetry), degrees
$\phi$	angle between span axis and horizontal, positive when right wing is down, degrees
$\psi$	angle between projection of resultant-force vector and projection of Z body axis in a horizontal plane, degrees
$\beta_{cg}$	approximate angle of sideslip at center of gravity (angle between relative wind and plane of symmetry at center of gravity), positive when relative wind comes from right of plane of symmetry, degrees
$\beta_t$	approximate angle of sideslip at tail (angle between relative wind and plane of symmetry at tail), positive when relative wind comes from right of plane of symmetry, degrees

## APPARATUS AND MODELS

## Apparatus

The rotary balance used for measuring the aerodynamic forces and moments on the  $\frac{1}{10}$ -scale model of a fighter airplane was designed for use in the Langley 20-foot free-spinning tunnel. This rotary balance system may be used to obtain data both in the spinning and normal flight range. A schematic diagram of the rotary balance system as installed in the tunnel is shown in figure 2. The rotating portion of the balance system, mounted on a horizontal supporting arm which is hinged at the wall, is moved from the wall to the center of the tunnel by cables and

winches. The rotary arm of the balance system, which rotates about a vertical axis, is attached at the outer end of the horizontal supporting arm and is driven by a drive shaft and appropriate linkages. The rate of rotation may be varied up to 200 rpm in either direction. Adjustable counterweights are attached to the upper end of the rotary arm to counterbalance the rotating parts. At the lower end of the rotary arm is a spin-radius setting arm that can be adjusted to simulate various radii from the center of rotation. At the end of the spin-radius setting arm is the model-attitude setting block to which the actual balance and model are attached. This block can be adjusted so as to simulate various angles of attack and sideslip of the model. The ranges of angles of attack and sideslip may be varied from 0° to 360°.

The balance consists of a six-component strain gage that measures normal, longitudinal, and lateral forces and rolling, pitching, and yawing moments about the body axes. The strain-gage balance is a small compact unit, as illustrated in figure 3, consisting of 12 strain-gage beams, 2 beams for each of the 6 components it measures. Storage batteries provide the direct current for the strain-gage balance system, and the voltage is measured and regulated at a control panel. The current from the storage batteries is transmitted to the rotating strain gages through a system of brushes and slip rings that are mounted above the rotary arm (fig. 2). Each pair of strain-gage beams is wired into a Wheatstone bridge circuit that is electrically balanced when no external loads are present. When an external load is applied, the strain-gage beams are deflected and, consequently, unbalance the bridge. The current flow resulting from the unbalanced bridge is transmitted back through the slip-ring - brush arrangement where it is measured on a calibrated microammeter.

#### Models

The  $\frac{1}{10}$ -scale model of the fighter airplane used on the rotary balance was constructed at the Langley Aeronautical Laboratory. This model was scaled up from the  $\frac{1}{20}$ -scale dynamic model for which the free-spinning results used herein were available. A three-view drawing of the  $\frac{1}{10}$ -scale model in its original configuration, with the flaps and landing gear retracted and the cockpit closed, is shown in figure 4. The full-scale dimensional characteristics of the fighter airplane simulated by the models are given in table I and the full-scale mass characteristics are given in table II. Figure 5 is a photograph of the  $\frac{1}{10}$ -scale model in the clean condition and figure 6 shows the model in the landing condition and in the condition with external fuel tanks installed. For the rotary-balance

tests, part of the fuselage of the  $\frac{1}{10}$ -scale model above the wing was cut away in order that the strain-gage balance could be mounted inside the fuselage. The strain-gage balance was located so that the axes about which the strain-gage balance measured forces and moments were coincident with the body axes of the model through the center-of-gravity position of the simulated airplane in the normal-loading clean condition. A photograph of the  $\frac{1}{10}$ -scale model mounted on the rotary balance is shown as figure 7. A photograph of the previously tested  $\frac{1}{20}$ -scale model spinning in the Langley 20-foot free-spinning tunnel is shown as figure 8.

#### TESTING TECHNIQUES

##### $\frac{1}{10}$ -Scale Model

The  $\frac{1}{10}$ -scale model was mounted on the rotary balance in the Langley 20-foot free-spinning tunnel at attitudes and with control settings corresponding to those for the spins obtained previously with the  $\frac{1}{20}$ -scale free-spinning model for various model conditions. The  $\frac{1}{20}$ -scale model had oscillated slightly in pitch, roll, and yaw while spinning, and the average values of  $\alpha$  and  $\phi$  were used in setting the attitude of the  $\frac{1}{10}$ -scale model.

The  $\frac{1}{10}$ -scale model was mounted on the rotary balance in such a manner that the Z body axis of the model passed through the spin axis, although in an actual fully developed spin, as obtained with the  $\frac{1}{20}$ -scale model, the resultant aerodynamic-force vector passes through the spin axis. The Z-axis of the model and the resultant aerodynamic-force vector are not exactly coincident.

The  $\frac{1}{10}$ -scale model was tested on the rotary balance with the spin radii calculated from the data measured for the free-spinning model by the approximate formula

$$R_s = \frac{g \cot \alpha}{\Omega^2}$$

The radii so calculated are only approximate in that the formula is based on the assumption that the resultant force lies along the Z-body axis.

The angular velocity about the spin axis and the rate of descent of the model observed in the free-spinning tests were used to calculate the spin coefficient  $\Omega b/2V$ . Preliminary tests of the model on the rotary balance indicated that at high rates of rotation vibrations of the rotary balance occurred and, accordingly, actual scale ratios of the higher rates of rotation as measured on the free-spinning model were not simulated. All tests were performed at the proper values of the spin coefficient  $\Omega b/2V$ , however. For simplicity a constant tunnel velocity was used for all tests and was chosen so that the values of  $\Omega$  required to obtain the proper values of the spin coefficient  $\Omega b/2V$  were below that at which vibration started. A brief investigation made to determine the force and moment coefficients at a specific value of  $\Omega b/2V$  but at different tunnel velocities indicated no noticeable effect within the range of velocities possible.

#### $\frac{1}{20}$ -Scale Model

The previously performed free-spinning tests of the  $\frac{1}{20}$ -scale model were conducted in the Langley 20-foot free-spinning tunnel, the operation of which is generally similar to that described in reference 10 for the Langley 15-foot free-spinning tunnel except that the model launching technique has been changed from launching with a spindle to launching by hand with spinning motion. The model was observed in fully developed spins, data were recorded, and recoveries were attempted generally by rapid full rudder reversal. A recovery is considered to be satisfactory if the model stops spinning in  $2\frac{1}{4}$  turns or less (reference 11). This value has been selected on the basis of full-scale-airplane spin-recovery data that have been available for comparison with corresponding model test results. Values of the spin parameters obtained were converted to corresponding full-scale values by methods described in reference 10.

#### TEST CONDITIONS

#### $\frac{1}{10}$ -Scale Model

Measurements were made of the aerodynamic forces and moments of the  $\frac{1}{10}$ -scale model for the model conditions, control configurations,

attitudes, and spin coefficients presented in table III, these conditions having previously been determined with the  $\frac{1}{20}$ -scale free-spinning model.

The normal maximum control deflections used in the investigation were:

Rudder, degrees . . . . .	$\pm 30$
Elevator, degrees . . . . .	$\pm 20$
Ailerons, degrees . . . . .	$\pm 14$
Flaps, degrees . . . . .	45

The intermediate control deflections used were:

Elevator $\frac{2}{3}$ up, degrees . . . . .	$\pm 1\frac{2}{3}$
Ailerons $\frac{2}{3}$ deflected, degrees . . . . .	$\pm 9\frac{1}{3}$
Ailerons $\frac{1}{3}$ deflected, degrees . . . . .	$\pm 4\frac{2}{3}$

For the clean condition referred to herein, the cockpit was closed, the landing gear was retracted, and the flaps were neutral. For the landing condition, the flaps were deflected  $45^\circ$  and the landing gear was extended. Tests were also performed with the flaps deflected  $45^\circ$  and the landing gear retracted.

The modified tail configurations shown in figures 9 to 12 were tested on the models. The tail-damping power factors (reference 11) of the models for the various modifications are presented in table IV.

As a result of the various model conditions, control configurations, and loadings, the investigation included large variations in spinning attitudes and spin coefficients, the angles of attack ranging from approximately  $20^\circ$  to  $70^\circ$ , the angles of sideslip at the center of gravity ranging from  $3^\circ$  inward to  $7^\circ$  outward, and spin coefficients  $\Omega b/2V$  ranging from 0.16 to 0.38.

All balance tests were made at a tunnel airspeed of 68.5 feet per second, which gives an approximate Reynolds number of 420,000 based on the mean aerodynamic chord of the  $\frac{1}{10}$ -scale model. This value of Reynolds number has not been corrected for the turbulence factor of the Langley 20-foot free-spinning tunnel, which is 1.8.

$\frac{1}{20}$ -Scale Model

The spinning attitudes and spin coefficients for each of the various model conditions and control configurations (table III) were obtained from previous tests of the  $\frac{1}{20}$ -scale model. The model had been spun arbitrarily to the right for the tests presented herein because brief tests performed to the left had shown that the model had symmetrical spin and recovery characteristics. As previously mentioned, the mass characteristics and mass parameters for loadings tested on the model are listed in table II. Loadings 2 and 3 were obtained on the  $\frac{1}{20}$ -scale dynamic model by installation of ballasted external fuel tanks. When the conditions for these loadings were tested on the  $\frac{1}{10}$ -scale model, geometrically similar external tanks were installed.

## CORRECTIONS

The forces and moments measured by the strain-gage balance were the sum of the aerodynamic forces and moments exerted on the  $\frac{1}{10}$ -scale model and the centrifugal forces and inertia moments produced by the rotation of the model and strain-gage beams. The centrifugal-force and inertia-moment values produced by the rotating model and strain-gage beams had to be subtracted from the values measured to obtain the aerodynamic values. In order to determine these corrections for each test, the centrifugal forces and inertia moments produced by the rotating model were calculated by using equations, presented in reference 1, derived from Euler's dynamical equations. When these equations are used, the weight, center of gravity, and moments of inertia of the model must be known; therefore, these values were measured for the  $\frac{1}{10}$ -scale model. The amounts of the centrifugal forces and inertia moments contributed by the strain-gage beams for each test were found experimentally.

Interaction of the forces and moments resulting from bending of the strain-gage beams when under load has been corrected for both in the measured aerodynamic characteristics and the calculated inertia tare corrections.

The effect of setting the  $\frac{1}{10}$ -scale model on the rotary balance at a value of spin radius that was approximate was examined and its influence was considered in analyzing the results.

The tunnel-wall effects were not considered significant since the model was located a large distance from the tunnel wall and the span of the model was small with relation to the tunnel diameter. Consideration of the interference between the model and the rotary balance indicated that the model might have been in the wake of the balance only for steep spinning angles of attack. For these steep spinning angles of attack, the tail of the model may have been in the wake of the rotary-balance arm; but inasmuch as the tail was a large distance behind the arm, where the wake disturbance was well-dissipated, no corrections were made for interference effects.

## ACCURACY

$\frac{1}{10}$ -Scale Model

The limits of accuracy of the measurements of the electrical strain-gage system are estimated to be as follows:

$C_x$	.....	$\pm 0.0082$
$C_y$	.....	$\pm 0.0033$
$C_z$	.....	$\pm 0.0127$
$C_l$	.....	$\pm 0.0007$
$C_m$	.....	$\pm 0.0011$
$C_n$	.....	$\pm 0.0004$

The limits of accuracy of the increments of the coefficients are believed to be somewhat better than the values listed.

The spin conditions set on the rotary balance simulated those measured on the free-spinning model within the following limits:

$\alpha$ , degrees	.....	$\pm 0.5$
$\phi$ , degrees	.....	$\pm 0.5$
$\Omega_b/2V$ , percent	.....	$\pm 1.5$

$\frac{1}{20}$ -Scale Model

The free-spinning results presented herein are believed to be the true values given within the following limits:

$\alpha$ , degrees	.....	$\pm 1$
$\phi$ , degrees	.....	$\pm 1$
$V$ , percent	.....	$\pm 5$
$\Omega$ , percent	.....	$\pm 2$
Turns for recovery, obtained from motion-picture records	.....	$\pm 1/4$

The limits of accuracy of the measurements of the mass characteristics of both the  $\frac{1}{10}$ - and  $\frac{1}{20}$ -scale models are believed to be as follows:

Weight, percent . . . . .	$\pm 1$
Center-of-gravity location, percent $\bar{c}$ . . . . .	$\pm 1$
Moments of inertia, percent . . . . .	$\pm 5$

#### PRESENTATION OF RESULTS

The aerodynamic force and moment coefficients as measured on the  $\frac{1}{10}$ -scale model are presented in table III. The free-spinning characteristics of the previously tested  $\frac{1}{20}$ -scale model are also presented in table III in terms of full-scale values. A comparison of the approximate spin radius used and the radius calculated from the measured resultant aerodynamic force is presented in table V. Also presented in table V are the values of the angle between the measured resultant aerodynamic force and the Z body axis when the angle is projected alternately into a horizontal plane ( $\psi$ ), into the XZ body plane, and into the YZ body plane. The effect of setting the rudder from with to against the spin on the aerodynamic force and moment coefficients of the  $\frac{1}{10}$ -scale model and the corresponding recovery characteristics of the  $\frac{1}{20}$ -scale model by rapid full rudder reversal are presented in table VI. The difference in aerodynamic yawing-moment coefficients between the rudder-with and rudder-against settings is plotted against angle of attack of the model in figure 13 and the total aerodynamic yawing-moment coefficient of the model with the rudder set against the spin is plotted in figure 14. The results of tests performed on the  $\frac{1}{10}$ -scale model with the horizontal tail in the original and rearward positions (fig. 9), with the spinning conditions held constant, are presented in table VII and show the effect on the aerodynamic force and moment coefficients of unshielding the vertical tail by movement of the horizontal tail. The increments of yawing-moment coefficients caused by rudder reversal for the two horizontal-tail positions are presented in table VIII and figure 15. The effect of deflecting the landing flaps on the aerodynamic moment coefficients is shown in table IX.

The inertia force and moment coefficients calculated for the fully developed spins are compared with the measured aerodynamic force and moment coefficients in table X.

## RESULTS AND DISCUSSION

A study of existing data (unpublished) of the spin characteristics of numerous models tested in the Langley free-spinning tunnels indicates that the range of spin conditions of the investigation presented herein is fairly wide and the results of the present investigation may therefore be taken as a general indication of the order of magnitude and direction of the aerodynamic forces and moments acting in normal fully developed spins of a straight-wing airplane with both vertical and horizontal tails.

## General Aerodynamic Characteristics in Spins

The results of the force and moment measurements (table III) show that, for the spins presented, the normal-force and longitudinal-force coefficients and the pitching-moment coefficients always had negative values. In other words, in an erect spin (positive angle of attack) the aerodynamic normal force always acted upward and toward the center of rotation, the aerodynamic longitudinal force always acted toward the rear of the airplane, and the aerodynamic pitching moment was always a nose-down moment as would normally be expected for a conventional airplane at a positive angle of attack. The nose-down aerodynamic pitching-moment coefficient and the upward normal-force coefficient increased as the angle of attack increased.

The results of the rolling-moment measurements presented herein and other unpublished data indicate that the ailerons were approximately one-half or less as effective in producing rolling-moment coefficients above the stall as below the stall. The rolling-moment coefficient, however, varied in the same manner with aileron deflection above and below the stall; that is, when the ailerons were set to simulate a stick position to the right (rotation to the right), a positive rolling-moment coefficient was generally obtained, and when the ailerons were set to simulate a stick position to the left, a negative rolling-moment coefficient was obtained. No consistent variation in the lateral-force coefficient resulting from the variations in the spinning conditions tested was noted. The aerodynamic yawing-moment coefficients as measured were always anti-spin (negative for the right spins presented), even with the rudder set full with the spin. For these tests, therefore, the sign of the yawing-moment coefficient is the same as the sign of the sideslip angle at the tail, which was always outward or negative for the right spins tested.

Relation of the Aerodynamic Characteristics to the Inertia  
Characteristics in Spins

In a fully developed spin, the aerodynamic forces and moments acting on an airplane must be balanced by the inertia forces and moments produced by the rotating mass of the airplane in order to obtain a condition of dynamic equilibrium. Components of the resultant of the normal, longitudinal, and lateral aerodynamic forces balance the weight and the centrifugal force of the rotating airplane. Similarly, the aerodynamic pitching moment balances the inertia pitching moment of the rotating airplane, and the aerodynamic rolling and yawing moments balance inertia rolling and yawing moments, respectively. The equations of the inertia and aerodynamic moments as presented in reference 14 from Euler's dynamical equations are as follows:

Rolling moment:

$$(I_Y - I_Z)qr - I_X \frac{dp}{dt} = -L$$

Pitching moment:

$$(I_Z - I_X)pr - I_Y \frac{dq}{dt} = -M$$

Yawing moment:

$$(I_X - I_Y)qp - I_Z \frac{dr}{dt} = -N$$

where

$$p = \Omega \cos \alpha$$

$$q = \Omega \sin \phi$$

$$r = \Omega \sqrt{\sin^2 \alpha - \sin^2 \phi}$$

These equations were developed for use about the principal axes of inertia but are used herein about the body axes. Possible discrepancies from using these equations about the body axes are considered to be negligible in that the angles between the body axes and principal axes are small.

In these equations, the values on the right-hand side of the equations are the aerodynamic moments that result from the motion of the airplane in a spin. The sum of the values on the left-hand side of the equations is the sum of the inertia moments. The terms of the inertia equations dependent on the time rate of change of  $p$ ,  $q$ , and  $r$  are the acceleration terms that would be zero in a completely steady spin. The values measured on the rotary balance are equal to the values on the right-hand side of the equations for steady spin conditions. As previously indicated, for the spins investigated, the free-spinning model oscillated slightly and the aerodynamic coefficients were measured for average values of the spin parameters determined in the free spins. The values of aerodynamic forces and moments as measured on the balance therefore appear to be approximate averages of the unsteady values existent in the actual spins.

Consideration of equations for equilibrium indicates certain conclusions regarding spinning equilibrium. For the pitching moment, the inertia effect depends on  $p$ ,  $r$ , and  $I_Z - I_X$ . The inertia pitching moment will always be positive because the value of  $I_Z - I_X$  is positive and  $p$  and  $r$  have the same sign and, therefore, their product will always be positive. For the attainment of equilibrium, the aerodynamic pitching moments must be negative. The values of aerodynamic pitching moment measured (table III) are all negative.

The sign of the inertia rolling moment depends on the signs of  $I_Y - I_Z$  and of the product of  $r$  and  $q$ . For normal designs  $I_Y - I_Z$  is always negative, and the product of  $r$  and  $q$ , which can change the sign of the inertia rolling moment, depends on whether the value of  $\sin \phi$  is positive or negative. As was previously noted (table III), the direction of the measured aerodynamic rolling moment changed and in general varied primarily with aileron position. The sign of  $\phi$  has been observed for tests of numerous models (unpublished data) and, as is indicated in table III, has been found to have a variation with aileron position similar to that for the measured aerodynamic rolling moment. In general, when the ailerons were with the spin (stick right in a right spin), the values of  $\phi$  were positive (table III); therefore the inertia rolling moments were negative, and positive aerodynamic rolling moments were needed for equilibrium. When the ailerons were with the spin, the measured aerodynamic rolling moments were positive (table III). Conversely, when the ailerons were against the spin, the values of  $\phi$  generally were negative and thus the inertia rolling moments were positive, and negative aerodynamic rolling moments were required for equilibrium.

With the ailerons against the spin, the measured aerodynamic rolling moments were generally negative.

An examination of the equilibrium equation for yawing moment indicates that the inertia yawing moment is dependent on the sign of  $\phi$ . Because the sign of  $\phi$  varied for the spins investigated (table III), the inertia yawing moment would also change sign. All the values of the measured aerodynamic yawing moments (table III), however, were negative (or anti-spin); consequently, when  $\phi$  was positive, the aerodynamic and inertia yawing moments were of like sign and the requisites for spinning equilibrium were not fulfilled. The  $\frac{1}{20}$ -scale model, however, actually spun for the cases presented herein and therefore had values of inertia moment coefficients equivalent to those calculated and presented in table X within fairly close limits. At least some of the measured aerodynamic yawing moments therefore may be in error.

Generally the measured aerodynamic yawing-moment coefficients were too large against the spin; thus the sideslip angles set on the rotary balance may have been too large outward. The fact that the radii set on the balance were only approximate (previously discussed) could account for some change in angle of sideslip. The differences between the approximate radii set on the rotary balance and radii calculated from the measured aerodynamic force coefficients (table V) indicate that the radii tested were generally larger than the actual radii of the spin. Examination of the equation for the sideslip at the center of gravity

$$\beta_{cg} = \phi - \tan^{-1} \frac{\Omega R_s \cos \psi}{V}$$

indicates that such a reduction in radius and any amount of the angle  $\psi$  (angle between the projection of the resultant-force vector and the projection of the Z body axis in a horizontal plane) would reduce the outward sideslip (or increase the inward sideslip) of the actual spin over that tested on the rotary balance. The differences in radii and the angle  $\psi$ , therefore, do account for some changes in angle of sideslip and therefore could account in part for some of the discrepancy in the measured aerodynamic yawing-moment coefficients.

Another factor that may be considered is that the inertia moment coefficients presented herein are based on the steady-state portion of Euler's equations and do not include the effect of any oscillations which may have existed on the free-spinning model. An integration of the effects of oscillations for one or more complete turns, however, would probably be zero and, as previously indicated, the data presented would be the average for one or more complete turns of the spin. Further

explanation of this lack of equilibrium between the aerodynamic and inertia yawing-moment coefficients is not readily available, and further study of this matter by iterative testing seems desirable.

As previously indicated, the measured aerodynamic yawing-moment coefficients were too large against the spin. Unpublished data of a contemporary investigation have indicated, however, that the instantaneous slopes of the variations of  $C_n$  with rudder deflection are approximately the same for each angle of attack above the stall, a result which is also generally true for the variation of  $C_n$  with sideslip angle and of  $C_n$  with spin coefficient. These results indicate that increments of measured aerodynamic yawing-moment coefficient  $\Delta C_n$  presented herein may be considered accurate even though the total aerodynamic yawing-moment coefficients are generally conservatively large.

The comparison of the aerodynamic forces and moments (table X) indicates slight differences in the rolling and pitching moments as well as the differences in yawing moments previously discussed. The differences in the rolling and pitching moments were generally in magnitude and not in sign, as was the case for the yawing moments. The differences in the rolling moments were used to determine incremental values of the angle  $\phi$  which, when used in Euler's dynamical equation, would account for the differences in the rolling moments. An average incremental value of  $\phi$  of approximately  $2.0^\circ$  was obtained for all tests and is not believed to be unreasonable if the over-all limits of the test procedures are considered. A change in  $\phi$  of this order of magnitude generally was not sufficient to influence the lack of equilibrium in the yawing-moment coefficients previously discussed.

The differences in the pitching moments were used to determine incremental values of the rate of rotation  $\Omega$  which, when used in Euler's dynamical equations for pitching moment, would account for the differences in pitching moments. An average incremental value of  $\Omega$  of approximately  $-0.12$  radian per second (full-scale) was obtained for all tests and is considered to be relatively small with regard to spinning.

To summarize, it has been indicated that the rolling-moment and pitching-moment coefficients and the increments in yawing-moment coefficients presented herein are relatively accurate. The total aerodynamic yawing moments, however, are generally too large against the spin, and therefore requirements based on the total aerodynamic yawing-moment coefficients are considered to be conservative.

### Effect of Rudder Reversal on Aerodynamic Coefficients

The results of spin-tunnel tests of numerous models have indicated that the rudder can normally be an effective control for recovery from spins. This fact is true particularly when the mass of the airplane is distributed primarily along the fuselage (references 11 and 13). Many current airplanes of rocket- and jet-propelled designs have this type of loading and most of the free-spinning tests, presented herein for comparison with balance data, were made with such a weight distribution.

Accordingly, the aerodynamic force and moment coefficients in a spin were determined when the rudder was set with the spin and when the rudder was set against the spin. The results of these tests are given in table VI in terms of the incremental differences in the moment and force coefficients with the rudder set with and against the spin. The primary effect of rudder reversal on the rigidly mounted  $\frac{1}{10}$ -scale model was a relatively large increment of anti-spin yawing-moment coefficient when compared with the aerodynamic yawing-moment coefficient that existed for the fully developed spin. The other force and moment coefficients were affected to only a small degree, the increments resulting from the change in rudder setting being relatively small when compared with the aerodynamic coefficients which existed in the fully developed spin. Reversal of the rudder on the free-spinning model generally resulted in immediate changes in model attitude and rate of rotation which initially resulted from changes in the forces and moments similar to those measured on the  $\frac{1}{10}$ -scale model.

The variation of the increment of yawing-moment coefficient with angle of attack is shown in figure 13 and indicates that below an angle of attack of approximately  $30^\circ$ , the value of the increment of the yawing-moment coefficient caused by rudder reversal is much larger than the value of the increment of yawing-moment coefficient obtained for spins above  $30^\circ$  angle of attack. The variation in rudder effectiveness with angle of attack appears to be primarily the result of the shielding of the rudder by the horizontal tail. Smoke-flow tests on a spinning airplane (reference 15) indicate the existence of such a shielding or blanketing effect of the horizontal tail on the vertical tail and rudder. A study of the tail-damping power factors and their components for the various tail configurations tested (table IV) and of the increments of yawing-moment coefficients caused by setting the rudder against the spin (table VI and fig. 13) indicates that at any given angle of attack the tail configuration that had the largest unshielded rudder volume coefficient consistently had the largest value of  $\Delta C_n$ . The trends indicated by the tail-damping power factor (reference 11) therefore seem to be in agreement with actual yawing-moment measurements in that the tail configurations having the largest calculated values of unshielded rudder volume coefficient had the largest values of  $\Delta C_n$  caused by rudder reversal.

The scatter of points or the variation of  $\Delta C_n$  at any given angle of attack shown in figure 13 is in part the result of these differences in rudder effectiveness. Also, at any given angle of attack, some scatter may result from a variation in sideslip for the various spin conditions tested for any given tail configuration.

Also indicated in figure 13 and table VI are those spins for which recoveries were satisfactory ( $2\frac{1}{4}$  turns or less) and those for which recoveries were not satisfactory by rudder reversal alone. The satisfactory recoveries generally were obtained by rudder reversal alone for spins in which  $\Delta C_n$  was of the magnitude of 0.012 or greater, against the spin. Such values of  $\Delta C_n$  were obtained only for spins in which the angle of attack was  $30^\circ$  or less. An exception was test 11 for which it was necessary to move the elevator as well as the rudder for satisfactory recovery. For test 11, the dynamic model was ballasted so that the weight was distributed primarily along the wings (loading 2, table II), and references 11, 12, and 16 indicate that for designs with the loading distributed primarily along the wings the elevator became the predominant control for recovery. For such loadings, therefore, in spite of the ability of the rudder to produce a large increment of anti-spin yawing moment, movement of the elevator for recovery may be essential.

#### Total Aerodynamic Yawing Moment Required to Obtain

##### Satisfactory Spin Recovery

A previous spin-balance investigation (reference 1) has indicated that an aerodynamic yawing-moment coefficient of the order of 0.020 against the spin would be required to be supplied by parts of the airplane (including interference effects) other than the wing to prevent equilibrium in a steady spin or to obtain recovery from a steady spin. A later paper (reference 3) indicates that a value of aerodynamic yawing-moment coefficient of 0.025 against the spin would be necessary to prevent equilibrium in a steady spin. Subsequent free-spinning-tunnel experience has indicated that spin and recovery requirements should be based on the

attainment of satisfactory spin recoveries ( $2\frac{1}{4}$  turns or less) and not just on recovery alone or the prevention of equilibrium in a spin because a design that has aerodynamic characteristics sufficient to prevent equilibrium in a steady spin may not be adequate for a satisfactory recovery. A requirement based on the amount of aerodynamic yawing-moment coefficient required to obtain satisfactory spin recovery therefore seems to be appropriate, and accordingly the following discussion is based on this premise. The results of force and moment measurements and of dynamic-model recovery tests were used to indicate the amount of total aerodynamic yawing-moment coefficient required for satisfactory recovery.

Because of discrepancies previously discussed, these results may be considered conservative. The brief study presented was confined to measurements made with the rudder set against the spin, in that recoveries were obtained only for this rudder setting. The requirements discussed are applicable only to designs with geometric configurations similar to and with mass distributions and relative densities of the same order of magnitude as the present configurations.

The total aerodynamic yawing-moment coefficients of the model with the rudder set against the spin for the various tests performed are presented in figure 14. Also shown in figure 14 are those cases for which satisfactory recoveries were obtained and those for which unsatisfactory recoveries were obtained. As is indicated in figure 13, recoveries from the spins at angles of attack of  $30^\circ$  or less were generally satisfactory. The maximum total aerodynamic yawing-moment coefficient against the spin existent for these satisfactory recoveries was of the order of magnitude of 0.021. From a conservative viewpoint, it would appear that a value of total aerodynamic yawing-moment coefficient ranging from approximately 0.021 to 0.025 (anti-spin) would be adequate for satisfactory recovery from steep spins. This value compares with that indicated from previous spin-balance work in that it was estimated from references 3 and 5 that the wing of the present investigation contributes very little to the total aerodynamic yawing-moment coefficient. A value ranging from 0.021 to 0.025 for steep spins appears, therefore, to be in agreement with the value previously indicated as required to be supplied by parts of the airplane other than the wing. The wing, however, may contribute a pro-spin aerodynamic yawing moment, as is generally indicated for steep spins (references 1, 3, and 5). The requirement presented herein for satisfactory spin recovery from steep spins therefore may be more stringent than the requirement indicated in previous spin-balance investigations for the prevention of equilibrium in a steady spin.

In general, satisfactory recoveries were not obtained above  $30^\circ$  angle of attack (fig. 14) although some spins having angles of attack greater than  $50^\circ$  had total yawing-moment coefficients of the same order of magnitude as those for which satisfactory recoveries were attained below  $30^\circ$  angle of attack. Because satisfactory recoveries generally were not obtained for spins at angles of attack above  $30^\circ$ , the data were not sufficient to determine the total amount of aerodynamic yawing-moment coefficient necessary for satisfactory recovery from any spin. It would appear, however, that the total aerodynamic yawing-moment coefficient against the spin required for satisfactory spin recovery may vary with angle of attack, increasing as the angle of attack increases, and that values larger than 0.025 may be required since values approaching 0.020 were obtained at high angles of attack for some of the cases presented herein and the recoveries were unsatisfactory. This fact further indicates that the previous requirement (references 1 and 3) is not applicable for satisfactory recoveries from spins.

Previous discussion of the increments of yawing-moment coefficient resulting from rudder reversal has indicated that for airplane loadings for which rudder movement is required for satisfactory recovery, an increment of aerodynamic yawing-moment coefficient of the order of 0.012 or greater may lead to satisfactory recovery for steep spins and the discussion indicates that a total aerodynamic yawing-moment coefficient of the order of 0.025, which was previously mentioned as being a conservative value, may lead to satisfactory recoveries for the same conditions. For flatter spins, however, and for loading conditions for which the rudder is the primary control for recovery (reference 11) it is not known whether a requirement for satisfactory recovery should be based on the increment of aerodynamic yawing-moment coefficient caused by rudder reversal or on the total aerodynamic yawing-moment coefficient. It appears, however, that in either case the amount of incremental or total aerodynamic yawing-moment coefficient required may increase with angle of attack; whereas the amount of yawing-moment coefficient available may generally decrease with angle of attack. Thus, the danger of a flat spin and the necessity for properly designing airplanes to obtain relatively steep spins are indicated.

#### Effect of Horizontal-Tail Position on Aerodynamic Coefficients

##### and Rudder-Reversal Effectiveness

Only one of the several tail modifications tested was effective in improving the spin-recovery characteristics of the original configuration. For the present study, the results for the other modifications were used only as means of extending the range of spinning attitudes for which data were made available. The effective modification (modification 1) was the one in which the horizontal tail was moved 15 inches (full-scale) rearward of the original position (fig. 9).

A study of the results of tests, in which force and moment measurements were made with the horizontal tail in both the original and revised positions for spinning attitudes obtained on the dynamic model with the original tail position (tables VII and VIII), indicates changes in the forces and moments to which the improvement in the spin and recovery characteristics obtained by the rearward horizontal-tail movement may be attributed. When the rudder was with the spin (table VII), moving the horizontal tail rearward led to an increase in the nose-down pitching-moment coefficient and to a slight decrease in the anti-spin yawing-moment coefficient. The effect of these aerodynamic changes for the free-spinning tests was generally to decrease the angle of attack of the spin for any given control configuration. The effect on the yawing-moment coefficient (table VII) is in general accord with the indications of tail-damping power factor (reference 11), a factor which is based on the tail geometric measurements and is used as an indication of the tail

power in effecting spin recovery. Calculations of tail-damping power factor for modification 1 (table IV) show a decrease in tail-damping ratio and an increase in unshielded rudder volume coefficient which would lead to a decrease in the anti-spin yawing-moment coefficient when the rudder was with the spin.

A comparison of the increments of yawing-moment coefficients resulting from rudder reversal for the model with the horizontal tail in the original position and with the horizontal tail moved rearward is presented in table VIII. When the horizontal tail was in the original position, the increments of yawing-moment coefficient were relatively small and in some cases were positive; this result may be attributed to some interference effects on the shielded rudder. When the horizontal tail was in the rearward position, the increments of yawing-moment coefficient were generally relatively large and negative (anti-spin). Inasmuch as only the horizontal tail was moved, the increase in the increment of anti-spin yawing moment due to reversing the rudder (or rudder-reversal effectiveness) was caused by the unshielding of the rudder. In order to illustrate further the increase in rudder-reversal effectiveness due to the unshielding of the rudder, a plot of incremental yawing-moment coefficient due to rudder reversal with the horizontal tail in the original position against the incremental yawing-moment coefficient obtained with the horizontal tail in the rearward position (fig. 15) shows that in all cases the greatest rudder-reversal effectiveness was obtained with the revised tail.

This investigation shows primarily the effect of unshielding the rudder in spinning attitudes. Movement of the horizontal tail rearward as was done in the present investigation may not necessarily unshield the rudder for other airplane tail designs.

#### Effects of Lowering Landing Gear and Deflecting Flaps on Spin

##### Attitudes and Aerodynamic Coefficients

The effects of lowering the landing gear and deflecting the flaps on the spin attitudes and aerodynamic force and moment coefficients are shown in table III. Only slight differences were obtained between the spin attitudes with the flaps deflected and landing gear down, and with only the flaps deflected. These results are in agreement with a complete study of the effects of landing gear and flaps on spin and recovery characteristics (reference 17) in that the landing gear has only a slight effect. The force measurements in table III also show little effect of the landing gear. The results of the free-spinning tests presented in table III, however, indicated an adverse effect of deflecting the flaps in that the spins were somewhat flatter when the flaps were deflected.

In order to study the effects of flaps on the rudder-reversal effectiveness, several tests were made on the balance with the model set at arbitrary attitudes and control settings. For each attitude and control setting, the flaps were deflected and retracted, and the results are presented in table IX. The increments of yawing-moment coefficient resulting from setting the rudder from with to against the spinning rotation were much larger when the flaps were up than when they were deflected; thus a definite adverse effect of flaps on the rudder was indicated. These results are in good agreement with the results of reference 17 which indicate an adverse effect of deflecting the flaps on recovery characteristics.

#### CONCLUSIONS

The following conclusions are based on the aerodynamic force and moment coefficients measured on a  $\frac{1}{10}$ -scale model of a fighter airplane in spinning conditions simulating those obtained previously for a similar dynamic model and in other arbitrary spinning conditions:

1. The primary effect of rudder reversal was to give a relatively large increment of anti-spin yawing-moment coefficient when compared with the aerodynamic yawing-moment coefficient of the fully developed spin. The other force and moment coefficients were affected to a much less degree.
2. The increment of yawing-moment coefficient obtained by rudder reversal in spins was much larger at low angles of attack than at high angles of attack; this result indicates that more rudder-reversal effectiveness was obtained in steep spins because of less rudder shielding.
3. Unshielding the rudder by movement of the horizontal tail rearward increased the rudder-reversal effectiveness.
4. Downward deflection of landing flaps reduced the rudder-reversal effectiveness.
5. A total aerodynamic yawing-moment coefficient ranging from approximately 0.021 to 0.025, anti-spin, may be required for satisfactory recoveries from steep spins based on a conservative estimate from the experimental results. Larger values of yawing-moment coefficient may be necessary for satisfactory recovery from flatter spins.

6. The aerodynamic force and moment measurements were in qualitative agreement with free-spinning results as regards spin and recovery characteristics.

Langley Aeronautical Laboratory

National Advisory Committee for Aeronautics

Langley Air Force Base, Va., June 16, 1950

## REFERENCES

1. Bamber, M. J., and Zimmerman, C. H.: Spinning Characteristics of Wings. I - Rectangular Clark Y Monoplane Wing. NACA Rep. 519, 1935.
2. Bamber, M. J.: Spinning Characteristics of Wings. II - Rectangular Clark Y Biplane Cellule: 25 Percent Stagger; 0° Decalage; Gap/Chord 1.0. NACA TN 526, 1935.
3. Bamber, M. J., and House, R. O.: Spinning Characteristics of Wings. III - A Rectangular and a Tapered Clark Y Monoplane Wing with Rounded Tips. NACA TN 612, 1937.
4. Bamber, M. J., and House, R. O.: Spinning Characteristics of Wings. IV - Changes in Stagger of Rectangular Clark Y Biplane Cellules. NACA TN 625, 1937.
5. Bamber, M. J., and House, R. O.: Spinning Characteristics of Wings. V - N.A.C.A. 0009, 23018, and 6718 Monoplane Wings. NACA TN 633, 1938.
6. Bamber, M. J., and Zimmerman, C. H.: Effect of Stabilizer Location upon Pitching and Yawing Moments in Spins as Shown by Tests with the Spinning Balance. NACA TN 474, 1933.
7. Bamber, M. J., and Zimmerman, C. H.: The Aerodynamic Forces and Moments Exerted on a Spinning Model of the "NY-1" Airplane as Measured by the Spinning Balance. NACA Rep. 456, 1933.
8. Bamber, M. J., and Zimmerman, C. H.: The Aerodynamic Forces and Moments on a Spinning Model of the F4B-2 Airplane as Measured by the Spinning Balance. NACA TN 517, 1935.
9. Bamber, M. J., and House, R. O.: Spinning Characteristics of the XN2Y-1 Airplane Obtained from the Spinning Balance and Compared with Results from the Spinning Tunnel and from Flight Tests. NACA Rep. 607, 1937.
10. Zimmerman, C. H.: Preliminary Tests in the N.A.C.A. Free-Spinning Wind Tunnel. NACA Rep. 557, 1936.
11. Neihouse, Anshal I., Lichtenstein, Jacob H., and Pepoon, Philip W.: Tail-Design Requirements for Satisfactory Spin Recovery. NACA TN 1045, 1946.
12. Neihouse, A. I.: Tail-Design Requirements for Satisfactory Spin Recovery for Personal-Owner-Type Light Airplanes. NACA TN 1329, 1947.

13. Stone, Ralph W., Jr., and Klinar, Walter J.: The Influence of Very Heavy Fuselage Mass Loadings and Long Nose Lengths upon Oscillations in the Spin. NACA TN 1510, 1948.
14. Webster, Arthur Gordon: The Dynamics of Particles and of Rigid, Elastic, and Fluid Bodies. Third ed., G. E. Stechert & Co. (New York), 1942, pp. 260-261.
15. Scudder, N. F., and Miller, M. P.: The Nature of Air Flow about the Tail of an Airplane in a Spin. NACA TN 421, 1932.
16. Neihouse, A. I.: A Mass-Distribution Criterion for Predicting the Effect of Control Manipulation on the Recovery from a Spin. NACA ARR, Aug. 1942.
17. Gale, Lawrence J.: Effect of Landing Flaps and Landing Gear on the Spin and Recovery Characteristics of Airplanes. NACA TN 1643, 1948.

TABLE I.- CORRESPONDING FULL-SCALE DIMENSIONAL  
CHARACTERISTICS OF A FIGHTER MODEL

Wing span, ft . . . . .	50.35
Length, over-all, ft . . . . .	44.70

**Wing:**

Area, sq ft . . . . .	425.0
Section, root . . . . .	NACA 65 <sub>112</sub> -213
Section, tip . . . . .	NACA 65 <sub>112</sub> -213
Root-chord incidence, deg . . . . .	2.5
Tip-chord incidence, deg . . . . .	2.5
Aspect ratio . . . . .	6.0
Sweepback of leading edge of wing, deg . . . . .	0
Dihedral, leading-edge chord line, deg . . . . .	6.0
Mean aerodynamic chord, in. . . . .	115.00
Leading edge of mean aerodynamic chord rearward of leading edge of wing, in. . . . .	0

**Flaps:**

Chord, percent of wing chord . . . . .	18.75
Area (rearward of hinge line), percent of wing area . . . . .	12.55
Span, percent of wing span . . . . .	44.0

**Ailerons:**

Chord, percent of wing chord . . . . .	20.00
Area (rearward of hinge line), percent of wing area . . . . .	5.90
Span, percent of wing span . . . . .	44.8

**Horizontal tail surfaces:**

Total area, sq ft . . . . .	108.0
Span, ft . . . . .	23.33
Elevator area (rearward of hinge line), sq ft . . . . .	30.0
Distance from normal center of gravity to elevator hinge line (original location of horizontal tail), ft . . . . .	22.95

**Vertical tail surfaces:**

Total area, sq ft . . . . .	36.0
Rudder area (rearward of hinge line), sq ft . . . . .	13.2
Distance from normal center of gravity to top of rudder hinge line, ft . . . . .	23.05



TABLE II.- CORRESPONDING FULL-SCALE MASS CHARACTERISTICS OF A FIGHTER MODEL

[Moments of inertia are given about center of gravity]

Loading	Weight (lb)	Center-of-gravity location		Relative airplane density, $\mu$		Moments of inertia (slug-ft <sup>2</sup> )			Mass parameters			
		x/c	z/c	Sea level	15,000 feet	I <sub>X</sub>	I <sub>Y</sub>	I <sub>Z</sub>	$\frac{I_X - I_Y}{mb^2}$	$\frac{I_Y - I_Z}{mb^2}$	$\frac{I_Z - I_X}{mb^2}$	
1	Normal	17,835	0.212	0.009	13.61	17.35	17,342	37,920	53,396	-147 $\times 10^{-4}$	-110 $\times 10^{-4}$	257 $\times 10^{-4}$
2	Full alternate loading	22,200	.200	.052	13.50	21.41	39,900	37,880	75,700	11	-215	204
3	Partial alternate loading	20,350	.200	.052	12.42	19.68	29,600	37,850	65,900	-47	-178	225
4	Center of gravity, 7 percent & rearward of normal	17,940	.282	.009	10.95	17.40	16,190	34,621	50,977	-130	-115	245

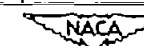


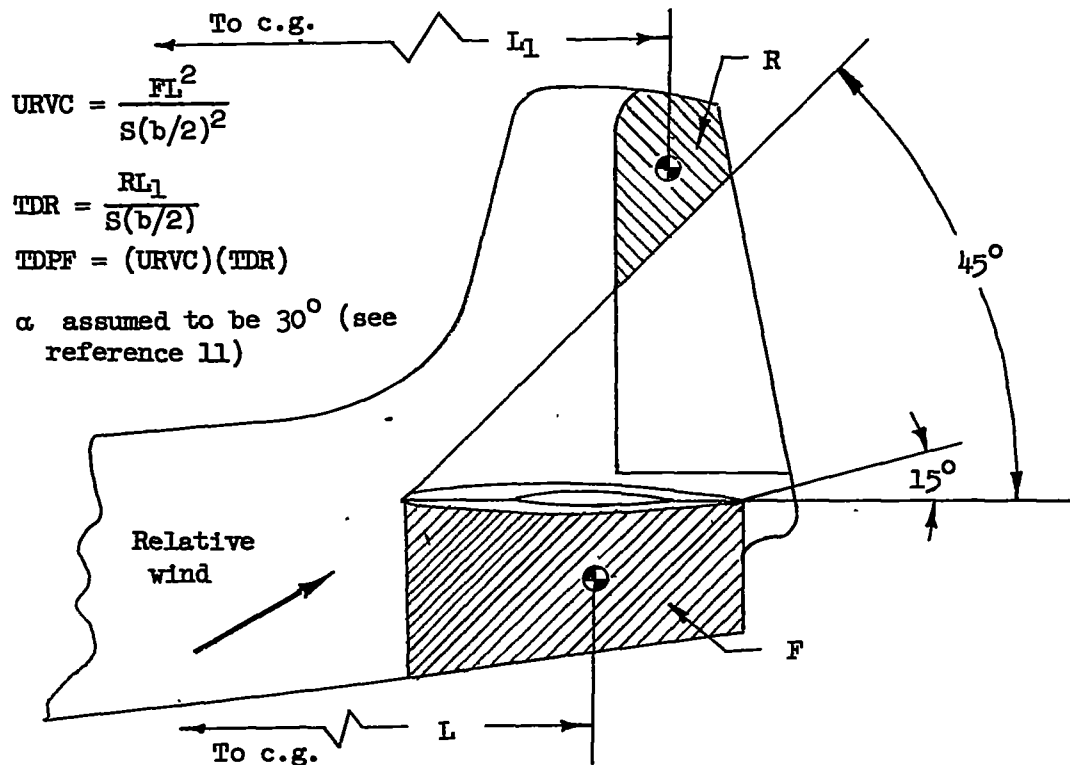
TABLE III.—FREE-SPINNING CHARACTERISTICS OF  $\frac{1}{20}$ -SCALE MODEL AND AERODYNAMIC FORCE AND MOMENT COEFFICIENTS OF  $\frac{1}{10}$ -SCALE MODEL OF A FIGHTER AIRPLANE IN SPINS

[Data have been converted to full-scale values; rudder full left; right crest spins]

Test	Modification	Figure (a)	Model condition	Loading condition (table II)	Control deflections		Free-spinning characteristics							Aerodynamic force and moment coefficients							
					Elevator	Ailerons	$\alpha$ (deg)	$\delta$ (deg)	$\beta_{eg}$ (deg)	$\beta_t$ (deg)	$\eta$ (rps)	$V$ (fps)	$R_b$ (ft)	$R_d$ (ft)	$C_x$	$C_y$	$C_z$	$C_l$	$C_m$	$C_n$	
1	None	Clean	1	Pull up	Pull against	46	-1.4	-2.2	-12.0	0.304	243	0.199	8.39	-0.0632	-0.0365	-1.2464	-0.0106	-0.0841	-0.0025		
2	do	do	1	Neutral	do	63	.6	-1.4	-14.5	.394	197	.316	8.69	-0.0254	-0.0365	-1.3715	-0.0011	-0.1697	-0.0087		
3	do	do	1	do	do	43	-3.6	-6.3	-17.3	.331	223	.234	8.08	-0.0446	-0.0276	-1.3882	-0.0106	-0.1107	-0.0051		
4	do	do	1	Pull down	do	42	-3.3	-6.1	-17.1	.414	210	.311	5.27	-0.0696	-0.0227	-1.4045	-0.0050	-0.1360	-0.0033		
5	do	do	1	Pull up	Neutral	50	2.0	-1.2	-14.4	.503	223	.256	2.71	-0.0220	-0.0443	-1.4459	-0.0013	-0.1076	-0.0068		
6	do	do	1	Neutral	do	35	.9	-4.4	-11.0	.358	243	.232	9.18	-0.0734	-0.0005	-1.1715	.0072	-0.0595	-0.0016		
7	do	do	1	Pull down	do	60	1.4	-1.0	-15.4	.372	190	.309	9.44	-0.0801	-0.0580	-1.6524	.0091	-0.1750	-0.0023		
8	1	Horizontal tail moved rearward	9	do	1	Pull up	Pull against	46	.4	-3.4	-13.3	.345	216	.252	6.68	-0.1040	-0.0303	-1.3346	-0.0072	-0.0861	-0.0033
9	2	do	9	do	1	Neutral	do	38	-1.4	-4.2	-12.6	.474	277	.272	4.58	-0.1070	-0.0114	-1.2334	-0.0111	-0.1010	-0.0046
10	1	do	9	do	1	Pull down	do	46	-.9	-3.9	-13.7	.400	240	.262	4.95	-0.0876	-0.0866	-1.4756	-0.0080	-0.1473	-0.0001
11	1	do	9	do	2	2/3 up	1/3 with	55	5.3	2.6	-3.7	.619	366	.268	4.48	-0.0767	-0.0344	-0.9308	.0015	-0.0268	-0.0042
12	1	do	9	do	3	Pull down	Pull with	34	3.0	.7	-7.7	.384	381	.269	3.53	-0.0804	-0.0400	-1.2370	.0060	-0.1247	-0.0059
13	1	do	9	do	3	Pull up	Pull against	22	.8	-3.7	-6.9	.422	379	.176	13.24	-0.0763	-0.0168	-0.8044	-0.0203	-0.0241	-0.0087
14	1	do	9	do	3	Pull down	do	24	-1.6	-5.8	-10.4	.482	353	.217	7.74	-0.0651	-0.0419	-1.1576	-0.0079	-0.1193	-0.0069
15	1	do	9	do	3	do	Neutral	22	-.1	-3.8	-8.4	.504	359	.244	6.59	-0.0635	-0.0410	-1.0930	.0079	-0.1109	-0.0011
16	1	do	9	do	4	Neutral	Pull against	24	-.5	1.1	-10.1	.539	334	.256	6.19	-0.0980	-0.0345	-0.9082	-0.0027	-0.0692	-0.0039
17	1	do	9	do	4	Pull down	do	26	-.5	-4.6	-10.6	.462	314	.243	7.38	-0.1037	-0.0348	-1.0883	.0009	-0.1028	-0.0094
18	1	do	9	Landing gear and flaps deflected $45^\circ$	1	Pull up	do	48	-2.1	-5.8	-16.0	.350	209	.264	6.05	-0.1377	-0.0233	-1.4608	-0.0046	-0.1118	-0.0057
19	1	do	9	do	1	Pull down	do	23	-1.7	-4.5	-16.3	.401	196	.382	3.81	-0.1425	-0.0844	-1.6697	-0.0011	-0.1504	-0.0059
20	1	do	9	do	1	Neutral	Neutral	50	1.6	-1.6	-12.1	.365	209	.373	5.06	-0.1800	-0.0494	-1.7785	.0059	-0.1493	-0.0002
21	1	do	9	do	1	Pull down	do	48	-3.3	-5.0	-19.7	.482	203	.373	3.10	-0.1501	-0.0163	-1.6536	.0051	-0.1766	-0.0042
22	1	do	9	Flaps deflected $45^\circ$	1	Pull up	Pull against	49	-3.2	-6.5	-19.3	.385	223	.230	6.78	-0.1998	-0.0254	-1.5977	-0.0003	-0.1123	-0.0069
23	1	do	9	do	1	Pull down	do	32	-1.3	-4.8	-17.3	.393	197	.315	4.08	-0.1438	-0.0418	-1.6689	-0.0066	-0.1177	-0.0024
24	1	do	9	do	1	Neutral	Neutral	45	.1	-2.9	-34.9	.403	197	.382	4.05	-0.2414	-0.0335	-1.5696	.0024	-0.1410	-0.0019
25	2 and 4	Small anti-spin fillets added to tail, fin and rudder extended up	10 and 11	Clean	1	Pull up	Pull against	53	-.3	-3.2	-13.0	.321	216	.235	5.46	-0.0477	-0.0320	-1.4334	.0010	-0.1104	-0.0158
26	3	Large anti-spin fillets added to tail	10	do	1	do	do	46	-3.1	-6.7	-16.0	.349	223	.247	6.31	-0.0823	-0.0297	-1.3112	-0.0013	-0.0856	-0.0146
27	3	do	10	do	1	do	2/3 against	50	2.0	-3.0	-5.2	.225	260	.162	13.50	-0.0589	-0.0455	-1.3398	-0.0056	-0.0967	-0.0068
28	4	Fin and rudder extended upwards	11	do	1	do	Pull against	64	1.6	-.3	-14.3	.384	197	.307	8.70	-0.0196	-0.0767	-1.4940	.0001	-0.1399	-0.0190
29	5	Fixed area added above fin and rudder	11	do	1	Neutral	do	67	.6	-1.2	-16.1	.378	150	.313	2.48	-0.0208	-0.0671	-1.6125	.0044	-0.1793	-0.0131
30	6	Area added to front of fin	11	do	1	Pull up	do	66	1.3	-.5	-13.7	.346	206	.264	3.08	-0.0009	-0.0639	-1.6055	.0020	-0.1549	-0.0182
31	7	Two ventral fins set at $45^\circ$ on fuselage	12	do	1	Neutral	do	41	-8.1	-4.8	-12.9	.433	288	.237	4.99	-0.0673	-0.0058	-1.2608	-0.0089	-0.2073	-0.0036
32	7	do	12	do	1	Pull down	do	45	-.4	-7.2	-19.4	.461	229	.331	3.04	-0.0690	-0.0206	-1.4256	-0.0032	-0.1845	-0.0077

Figure in which modification is shown.

TABLE IV.- TAIL-DAMPING POWER FACTORS FOR THE VARIOUS TAIL  
CONFIGURATIONS TESTED ON A FIGHTER MODEL



Modification	Figure (a)	Unshielded rudder volume coefficient, URVC (b)	Tail-damping ratio, TDR (b)	Tail-damping power factor, TDPF (b)
None		0.00948	0.0292	0.000277
1	9	.01500	.0243	.000364
2	10	.00948	.0454	.000431
3	10	.00948	.0464	.000440
4	11	.01870	.0292	.000546
5	11	.00948	.0292	.000277
6	11	.00948	.0292	.000277
7	12	.00948	.0288	.000273

<sup>a</sup>Figure in which modification is shown.

<sup>b</sup>Value as computed by methods of reference 11.



TABLE V.- COMPARISON OF APPROXIMATE SPIN RADII AND SIDESLIP  
 ANGLES TESTED AND SPIN RADII AND SIDESLIP ANGLES  
 CALCULATED FROM MEASURED AERODYNAMIC FORCES

Test	$R_s$ (ft)	$R_s$ (ft)	$\psi$ (a)	$\beta_{cg}$ (a)	$\beta_{cg}$ (a)	Angles between the Z body axis and resultant force (a)	
						Angle in XZ-plane	Angle in YZ-plane
1	8.53	7.57	0	-5.2	-4.8	3.1	1.7
2	2.69	2.24	-4.9	-1.4	-1.0	.9	2.3
3	8.08	4.61	0	-6.5	-6.1	1.9	1.2
4	5.27	2.37	0	-6.1	-5.0	2.8	1.1
5	2.71	2.58	0	-.2	-.1	2.1	2.2
6	9.18	4.64	0	-4.4	-2.0	3.6	0
7	3.44	2.11	-5.0	-1.0	-.1	.7	2.0
8	6.62	3.30	-1.7	-3.4	-1.5	4.5	1.3
9	4.58	4.95	0	-4.2	-4.5	4.9	.5
10	4.95	5.80	0	-3.9	-4.4	3.4	1.0
11	4.48	3.16	3.1	2.6	3.4	4.8	2.1
12	3.53	3.59	-3.0	.7	-.6	3.8	1.9
13	11.24	6.92	0	-3.7	-2.0	5.4	.8
14	7.74	6.99	2.6	-5.4	-5.0	4.3	2.1
15	6.59	4.99	2.8	-3.8	-2.9	3.5	2.2
16	6.19	4.77	2.2	-4.1	-3.3	5.3	2.0
17	7.32	5.72	2.7	-4.6	-3.7	5.4	1.8
18	6.05	3.66	0	-5.8	-4.3	6.2	.1
19	3.81	2.84	-3.3	-4.5	-3.8	4.9	.8
20	5.06	4.38	-3.9	-1.6	-1.2	4.6	1.6
21	3.10	2.44	0	-5.0	-4.4	5.2	.5
22	6.78	6.47	2.3	-6.8	-6.6	7.6	1.0
23	4.08	3.00	-3.1	-4.2	-3.5	4.9	1.5
24	4.05	2.10	-2.8	-2.9	-1.4	5.2	1.2
25	5.46	5.09	0	-3.2	-3.0	1.9	.1
26	6.51	3.97	0	-6.7	-5.3	3.6	1.3
27	13.50	9.28	-3.7	-3.0	-1.4	2.3	2.0
28	2.70	1.43	-6.7	-.3	-.6	.8	3.0
29	2.48	1.55	-6.3	-1.2	-.5	.4	3.1
30	3.02	4.72	-2.8	-.5	-1.6	0	2.3
31	4.99	6.85	-1.7	-4.8	-5.8	3.1	.3
32	3.64	3.10	0	-7.2	-6.7	2.8	.4

<sup>a</sup>Values based on the measured aerodynamic forces.



TABLE VI.-- THE EFFECT OF RUDDER REVERSAL ON THE NUMBER OF TURNS FOR RECOVERY AND ON THE AERODYNAMIC FORCE AND MOMENT COEFFICIENTS OF A FIGHTER MODEL IN A SPIN

[Coefficient increments obtained by setting the rudder from full left to full right against the spin; recoveries attempted by rapid full rudder reversal except as indicated.]

Test	$\frac{1}{10}$ -scale model						$\frac{1}{20}$ -scale model
	$\Delta C_x$	$\Delta C_y$	$\Delta C_z$	$\Delta C_l$	$\Delta C_m$	$\Delta C_n$	
1	-0.0016	-0.0059	-0.002	0.0015	-0.0011	0.0028	>10
2	.0068	-.0001	.010	.0007	-.0054	-.0014	>11
3	.0031	.0013	-.012	.0022	-.0036	.0031	>9
4	-.0005	.0048	-.018	.0022	-.0046	-.0027	>8
5	.0019	.0118	.012	.0003	-.0001	-.0007	>4
6	.0021	-.0038	-.033	.0010	-.0029	-.0030	$1\frac{1}{4}, 1\frac{1}{2}$
7	.0097	0	.006	.0008	-.0078	-.0009	>2, >2 $\frac{3}{4}$
8	.0048	.0148	-.011	.0017	-.0014	-.0047	$1\frac{1}{2}, 1\frac{3}{4}$
9	.0036	.0100	.014	.0012	-.0026	-.0055	2, $2\frac{1}{4}$
10	-.0035	.0165	.015	.0013	-.0018	-.0053	4
11	-.0070	.0290	.017	.0004	.0052	-.0119	>3, >3 $\frac{3}{4}, 1\frac{1}{4}, 1\frac{3}{4}$
12	-.0071	.0226	-.032	.0031	-.0030	-.0069	$2\frac{3}{4}$
13	-.0066	.0330	.045	.0018	.0062	-.0120	$\frac{1}{4}$
14	-.0054	.0478	.016	.0031	.0084	-.0179	$1\frac{1}{2}, 2$
15	-.0090	.0501	.020	.0020	.0067	-.0196	$1\frac{1}{4}$
16	-.0102	.0422	.029	.0013	.0121	-.0166	1, 1
17	0	.0432	.038	.0028	.0089	-.0161	$1\frac{1}{2}, 2\frac{3}{4}$
18	.0002	-.0034	-.010	.0042	-.0004	.0038	>11
19	.0065	.0012	-.006	.0002	-.0052	-.0024	>14
20	.0021	.0049	.023	.0014	-.0077	-.0021	6, 6
21	.0004	.0115	-.058	.0013	-.0088	-.0040	8
22	.0084	-.0070	.023	.0033	-.0001	-.0008	>8 $\frac{3}{4}$
23	.0153	.0066	-.003	.0008	-.0003	-.0030	>9
24	.0069	.0092	-.034	.0022	-.0070	-.0032	>10
25	.0015	-.0031	.008	.0003	.0018	.0003	>3
26	0	-.0010	.010	.0003	.0008	.0032	>8
27	0	-.0021	-.006	.0007	-.0006	.0017	>10
28	.0011	.0024	.011	.0011	-.0003	-.0043	>5
29	.0004	-.0005	-.019	.0004	-.0038	-.0012	>13
30	.0009	-.0006	.083	.0007	.0020	.0009	>5
31	.0052	.0006	-.025	.0011	-.0084	-.0011	$2, 2\frac{1}{4}$
32	.0015	-.0058	.012	.0015	-.0070	-.0018	>10

<sup>a</sup>Recovery attempted by simultaneous reversal of rudder from full left to 2/3 against the spin and elevator from 2/3 up to 1/3 down.

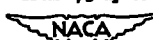


TABLE VII.- THE EFFECT OF UNSHIELDING THE VERTICAL TAIL BY  
HORIZONTAL-TAIL MOVEMENT ON THE AERODYNAMIC FORCE AND  
MOMENT COEFFICIENTS OF A FIGHTER MODEL IN A SPIN

[Coefficient increments obtained by moving the horizontal tail 15 in. (full-scale) rearward from the original position; rudder full with the spin]

Test	$\Delta C_x$	$\Delta C_y$	$\Delta C_z$	$\Delta C_l$	$\Delta C_m$	$\Delta C_n$
1	-0.0016	-0.0176	0.018	-0.0162	-0.0018	0.0005
3	-.0064	.0037	.010	-.0026	-.0040	.0007
25	-.0990	.0053	-.045	-.0020	-.0130	.0036
26	-.0300	.0004	-.022	-.0027	-.0046	.0041
27	-.0102	.0017	-.019	-.0011	-.0094	.0020
28	-.0240	.0069	-.074	-.0017	-.0189	.0025
29	-.0210	.0198	-.026	-.0021	-.0155	-.0039
30	-.0264	.0164	.053	.0035	-.0067	.0035
31	-.0189	.0077	-.070	-.0028	-.0128	-.0039
32	-.0415	.0208	-.058	.0038	-.0096	-.0069



TABLE VIII.- THE EFFECT OF UNSHIELDING THE VERTICAL TAIL  
ON RUDDER-REVERSAL EFFECTIVENESS ON A  
FIGHTER MODEL IN A SPIN

[Coefficient increments obtained by reversing the rudder  
from full with to full against the spin]

Test	Horizontal tail in original position		Horizontal tail in rearward position	
	$\Delta C_Y$	$\Delta C_n$	$\Delta C_Y$	$\Delta C_n$
1	-0.0059	0.0028	0.0083	-0.0031
3	.0013	.0031	.0123	-.0040
25	-.0031	.0003	0	-.0016
26	-.0010	.0032	.0012	-.0006
27	-.0021	.0017	.0009	.0003
28	.0024	-.0043	.0233	-.0088
29	-.0005	-.0012	.0053	-.0037
30	-.0006	.0009	.0066	-.0024
31	.0006	-.0011	.0107	-.0053
32	-.0058	-.0018	.0171	-.0027



TABLE IX.- EFFECT OF LANDING FLAPS ON THE YAWING-MOMENT-COEFFICIENT INCREMENTS DUE TO  
SETTING THE RUDDER FROM FULL WITH TO FULL AGAINST THE SPIN ON A FIGHTER MODEL  
[Horizontal tail moved 15 in. rearward (full-scale)]

Elevator deflection	Aileron deflection	$\frac{1}{20}$ -scale-model free-spinning results			$\frac{1}{10}$ -scale-model aerodynamic yawing-moment coefficient					
		$\alpha$ (deg)	$\phi$ (deg)	$\frac{\Omega b}{2V}$	Flaps neutral			Flaps $45^\circ$ down		
					Rudder with	Rudder against	$\Delta C_n$	Rudder with	Rudder against	$\Delta C_n$
Full up	Full against	46	0.4	0.252	-0.0034	-0.0081	-0.0047	-0.0046	-0.0030	0.0016
Neutral	--do--	38	-1.4	.272	-.0046	-.0101	-.0055	.0030	0	-.0030
Full down	--do--	46	-.9	.262	-.0002	-.0055	-.0053	.0027	-.0006	-.0033
Full down	--do--	52	-1.3	.315	-.0041	-.0095	-.0054	-.0024	-.0054	-.0030
Full up	Neutral	25	5.3	.268	-.0075	-.0167	-.0092	-.0104	-.0132	-.0028
Neutral	Neutral	45	.1	.322	-.0074	-.0116	-.0042	-.0019	-.0051	-.0032
Full up	--do--	25	-3.2	.268	-.0090	-.0213	-.0123	-.0114	-.0164	-.0050
Full up	--do--	52	5.3	.315	-.0042	-.0077	-.0035	-.0079	-.0101	-.0022
Full up	--do--	52	-1.3	.315	-.0102	-.0147	-.0045	-.0109	-.0117	-.0008

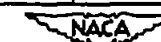
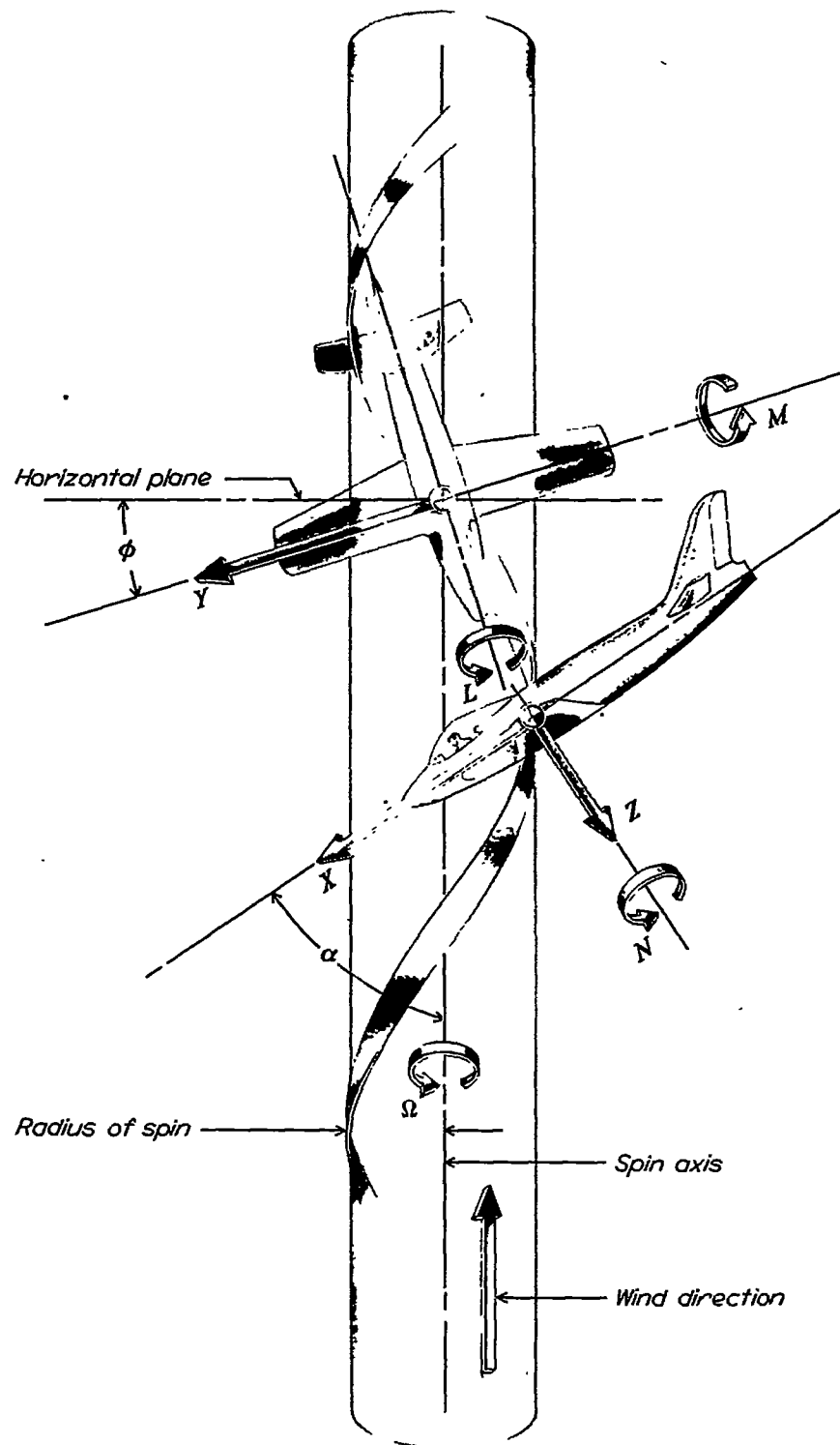


TABLE I.- COMPARISON OF THE RESULTANT INERTIA AND AERODYNAMIC FORCE COEFFICIENTS AND OF  
THE INERTIA AND AERODYNAMIC MOMENT COEFFICIENTS OF A FIGHTER MODEL IN A SPIN

Run	$\alpha$ (deg)	$\phi$ (deg)	$C_R$			$C_l$			$C_m$			$C_n$		
			Inertia	Aerodynamic	Difference									
1	46	-1.4	1.321	1.249	0.072	0.0012	-0.0106	0.0094	0.0705	-0.0841	0.0136	0.0013	-0.0025	0.0012
2	63	.6	1.622	1.574	.048	-.0016	-.0011	.0027	.1479	-.1697	.0818	-.0009	-.0087	.0096
3	43	-3.6	1.654	1.330	.324	.0041	-.0106	.0065	.1009	-.1107	.0098	.0049	-.0051	.0002
4	42	-3.3	1.900	1.426	.474	.0055	-.0050	-.0015	.1758	-.1360	-.0398	.0079	-.0033	-.0046
5	50	2.0	1.472	1.447	.025	-.0099	-.0013	.0072	.2293	-.1076	-.1217	-.0075	-.0068	.0123
6	35	.5	1.656	1.174	.482	-.0007	.0075	-.0070	.0922	-.0895	-.0057	-.0008	-.0016	.0024
7	60	1.4	1.795	1.653	.140	-.0036	.0091	-.0055	.1534	-.1720	.0216	-.0023	-.0053	.0076
8	46	.4	1.671	1.340	.331	-.0006	-.0072	.0078	.1178	-.0881	-.0297	-.0006	-.0033	.0039
9	38	-1.4	1.205	1.258	-.053	.0020	-.0111	.0091	.1336	-.1010	-.0326	.0028	-.0046	.0018
10	46	-.9	1.354	1.480	.126	.0014	-.0080	.0066	.1872	-.1475	.0203	.0015	-.0001	-.0014
11	25	5.3	1.030	.935	.095	-.0103	.0015	.0088	.0677	-.0588	-.0149	.0012	-.0042	.0030
12	34	3.0	1.088	1.220	.132	-.0020	.0060	-.0040	.1073	-.1247	.0174	.0007	-.0059	.0052
13	22	.8	.957	.809	.148	-.0005	-.0103	.0108	.0116	-.0841	.0125	-.0003	-.0087	.0030
14	24	-1.6	1.048	1.142	-.094	.0015	-.0079	.0064	.0341	-.1193	.0852	.0009	-.0089	.0020
15	22	-.1	1.127	1.056	.071	.0001	-.0079	-.0080	.0433	-.1109	.0676	.0001	-.0011	.0010
16	24	-.5	1.010	.995	.015	.0004	-.0027	.0023	.1000	-.0691	-.0309	.0001	-.0019	.0018
17	26	-.5	1.090	1.094	-.004	.0004	-.0009	-.0013	.0957	-.1053	.0096	.0008	-.0034	.0026
18	48	-2.1	1.728	1.470	.258	.0034	-.0046	.0012	.1286	-.1118	-.0168	.0033	-.0067	.0034
19	53	-1.7	1.828	1.678	.150	.0044	-.0011	-.0033	.1848	-.1804	-.0044	.0036	-.0029	-.0007
20	50	1.6	1.676	1.586	.090	-.0029	.0055	-.0026	.1377	-.1493	.0116	-.0026	-.0002	.0028
21	48	-2.3	1.832	1.659	.173	.0075	.0051	-.0126	.2988	-.1766	-.0822	.0072	-.0042	-.0030
22	49	-3.2	1.495	1.475	.020	.0039	-.0003	-.0036	.0971	-.1123	.0152	.0038	-.0089	.0051
23	52	-1.3	1.835	1.666	.169	.0032	-.0026	-.0006	.1782	-.1177	-.0605	.0027	-.0024	-.0003
24	45	.1	2.045	1.571	.474	-.0002	.0024	-.0022	.1925	-.1410	-.0515	-.0003	-.0019	.0022
25	55	-.3	1.030	1.434	-.404	-.0004	.0010	-.0006	.0959	-.1104	.0145	.0003	-.0158	.0155
26	46	-3.1	1.468	1.315	.153	.0042	-.0013	-.0029	.1129	-.0856	-.0273	.0044	-.0146	.0102
27	50	2.0	1.568	1.342	.226	-.0012	-.0096	.0108	.0480	-.0967	.0487	-.0012	-.0068	.0080
28	64	1.6	1.513	1.496	.017	-.0042	.0001	.0041	.1378	-.1399	.0021	-.0022	-.0130	.0152
29	67	.6	1.512	1.614	-.102	-.0017	.0044	-.0027	.1386	-.1793	.0467	-.0008	-.0131	.0139
30	66	1.3	1.609	1.610	-.001	-.0026	.0020	.0006	.0955	-.1549	.0594	-.0012	-.0182	.0194
31	41	-2.1	1.688	1.264	.424	-.0024	-.0029	.0005	.1032	-.1073	.0041	.0030	-.0036	.0006
32	45	-4.4	1.448	1.427	.021	.0105	-.0032	-.0073	.2023	-.1445	-.0778	.0115	-.0077	-.0038

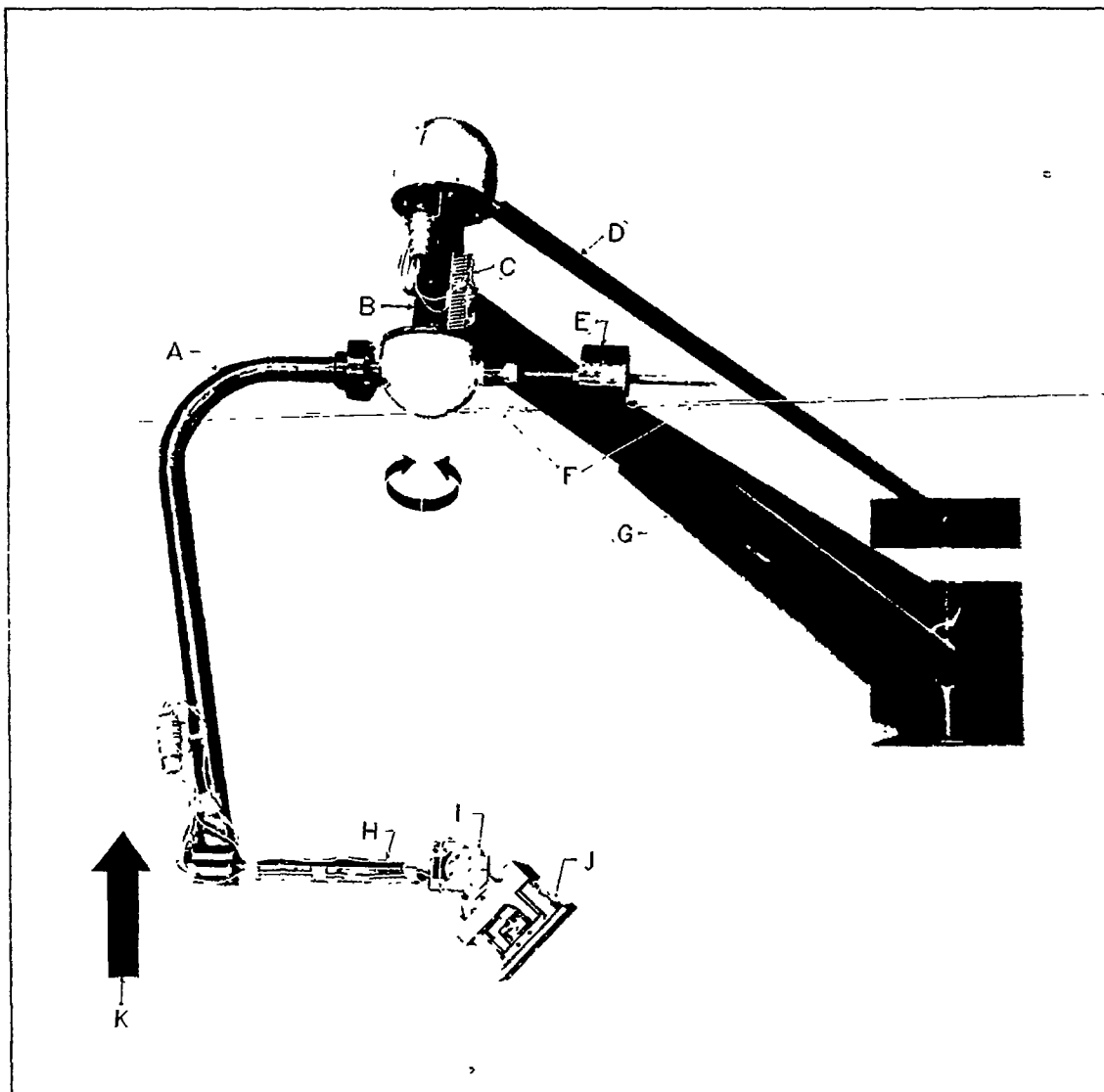
NACA



NACA  
L-64907

Figure 1.- Illustration of an airplane in a steady spin. Arrows indicate positive directions of forces and moments along and about the body axes of the airplane.



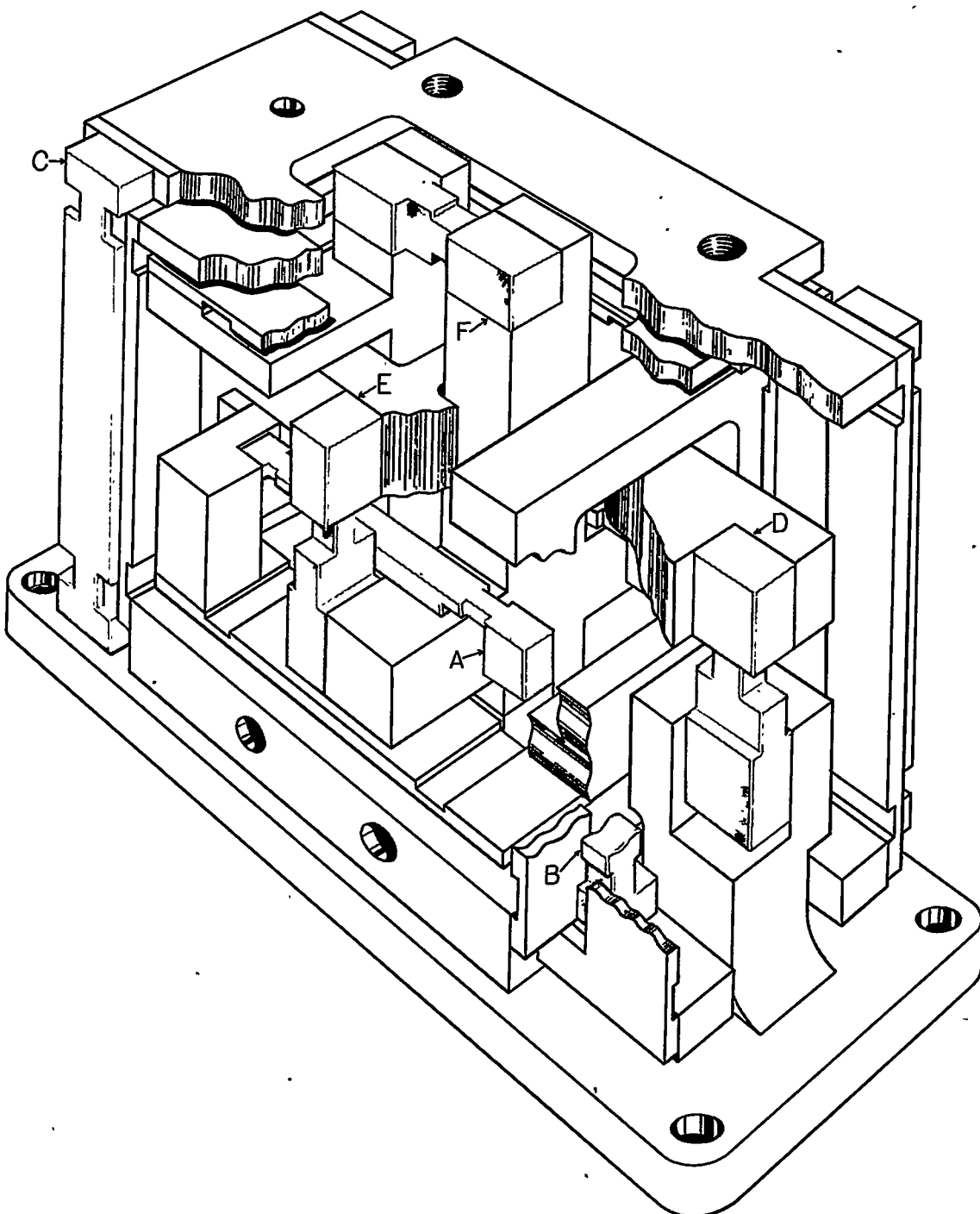


- |   |                        |   |                              |
|---|------------------------|---|------------------------------|
| A | Rotary arm             | F | Cables                       |
| B | Vertical member        | G | Horizontal supporting arm    |
| C | Slip rings and brushes | H | Spin-radius setting arm      |
| D | Drive shaft            | I | Model-attitude setting block |
| E | Counterweights         | J | Strain-gage balance          |
|   |                        | K | Wind direction               |

NACA  
L-64905

Figure 2.- The rotary balance in the Langley 20-foot free-spinning tunnel.





- A Normal-force beam
- B Longitudinal-force beam
- C Lateral-force beam
- D Rolling-moment beam
- E Pitching-moment beam
- F Yawing-moment beam



L-64906

Figure 3.- Illustration of the six-component strain-gage balance.



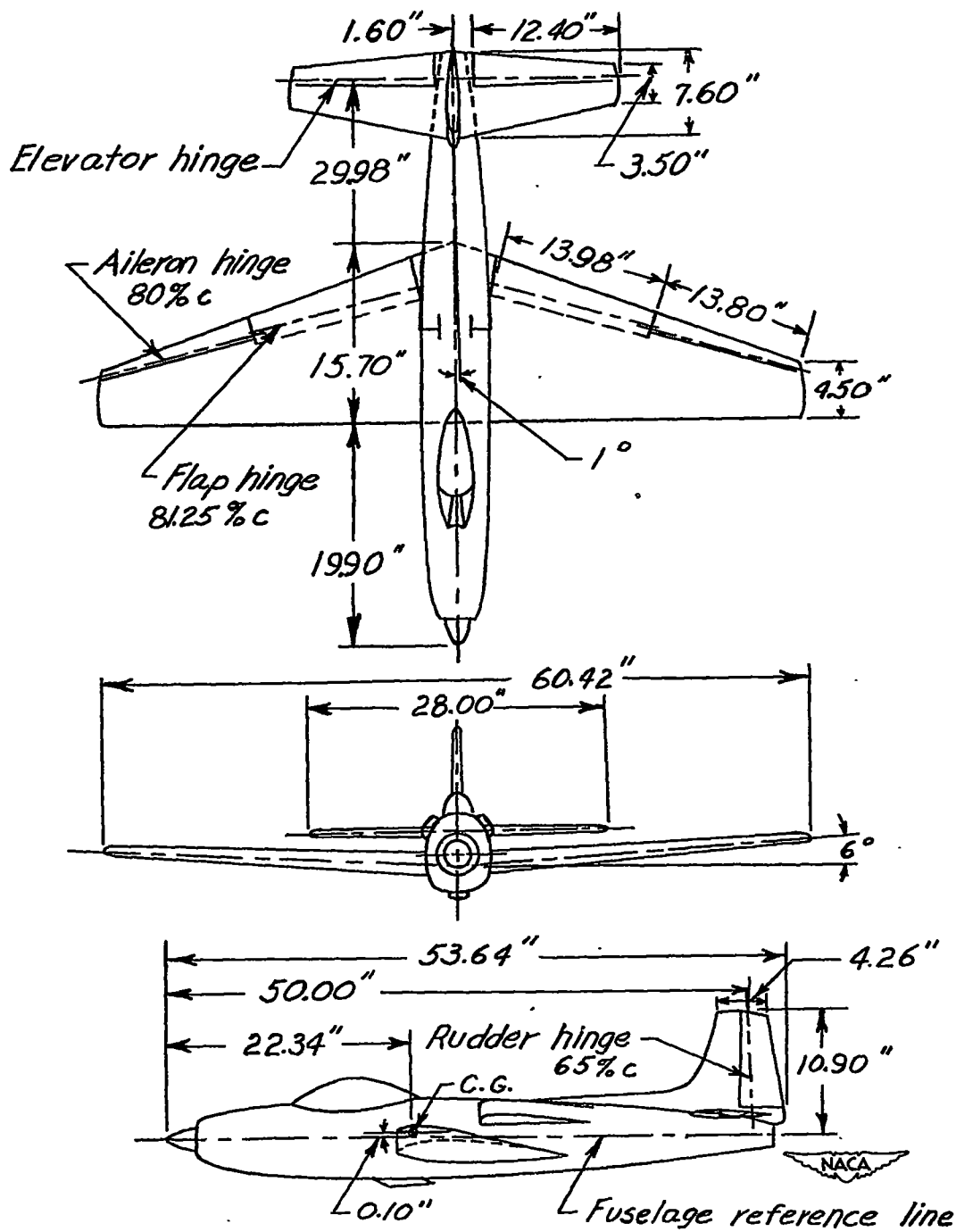


Figure 4.- Drawing of the  $\frac{1}{10}$ -scale model of a fighter airplane as tested on the rotary balance. Wing incidence,  $2\frac{1}{2}^{\circ}$  leading edge up; stabilizer incidence,  $1^{\circ}$  leading edge up. Center-of-gravity position shown for normal loading.



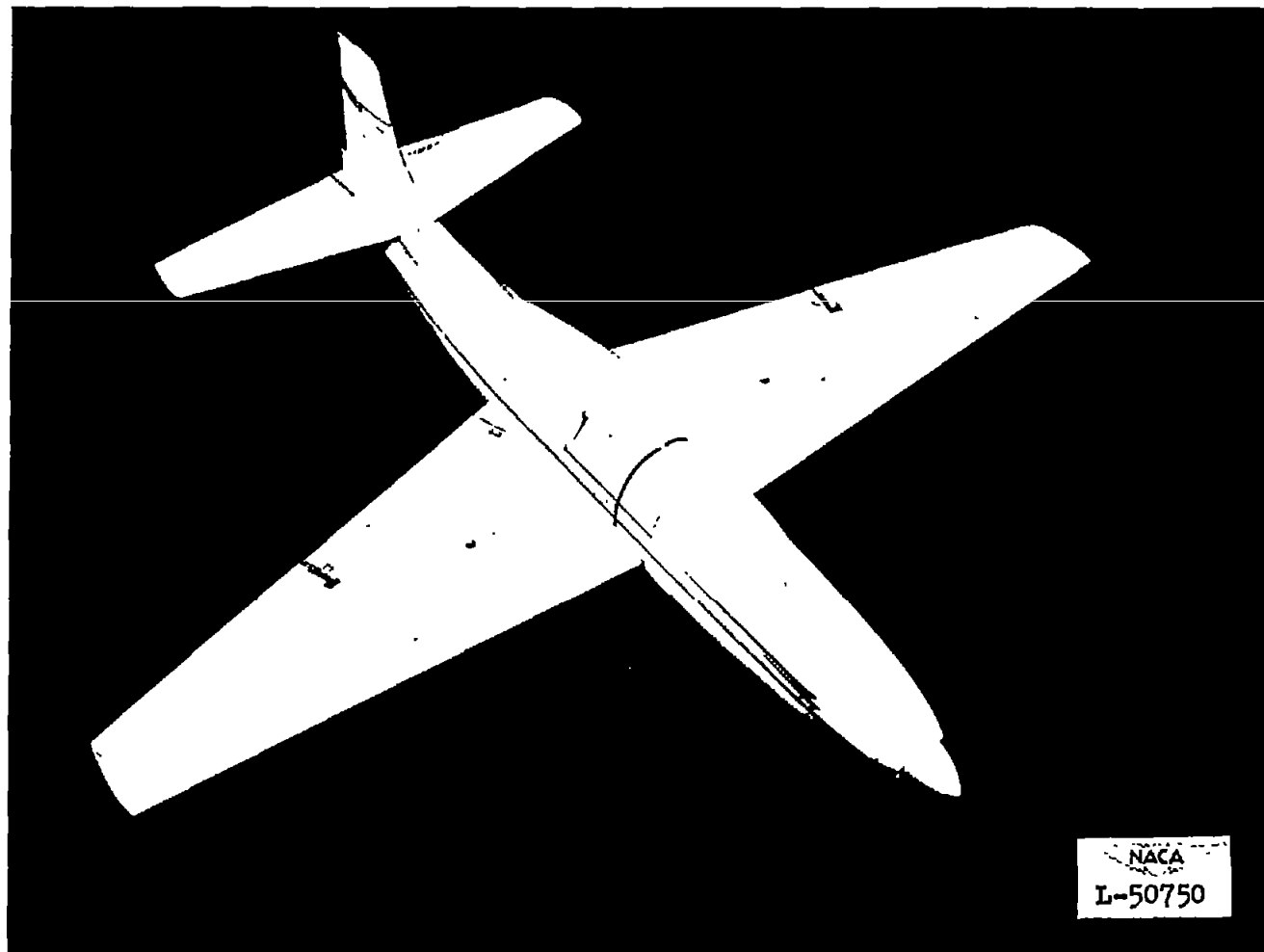
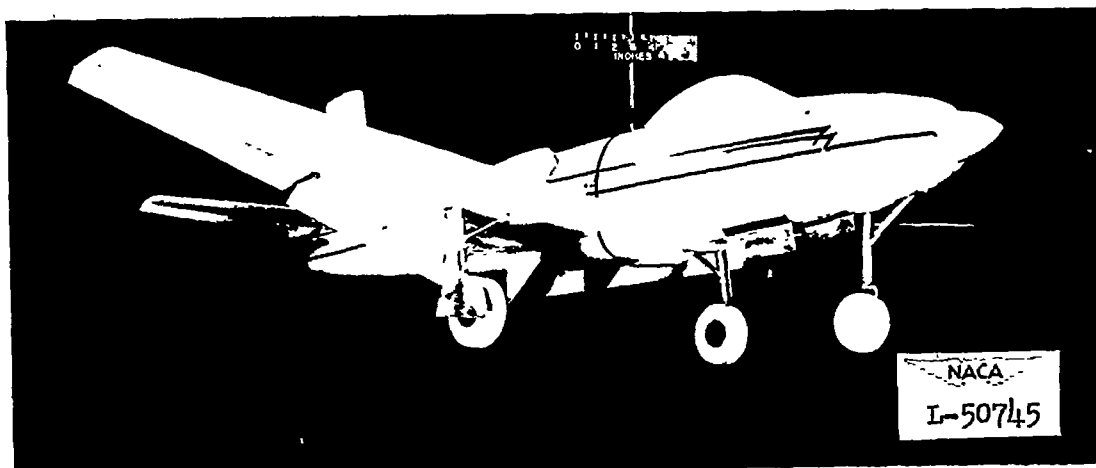
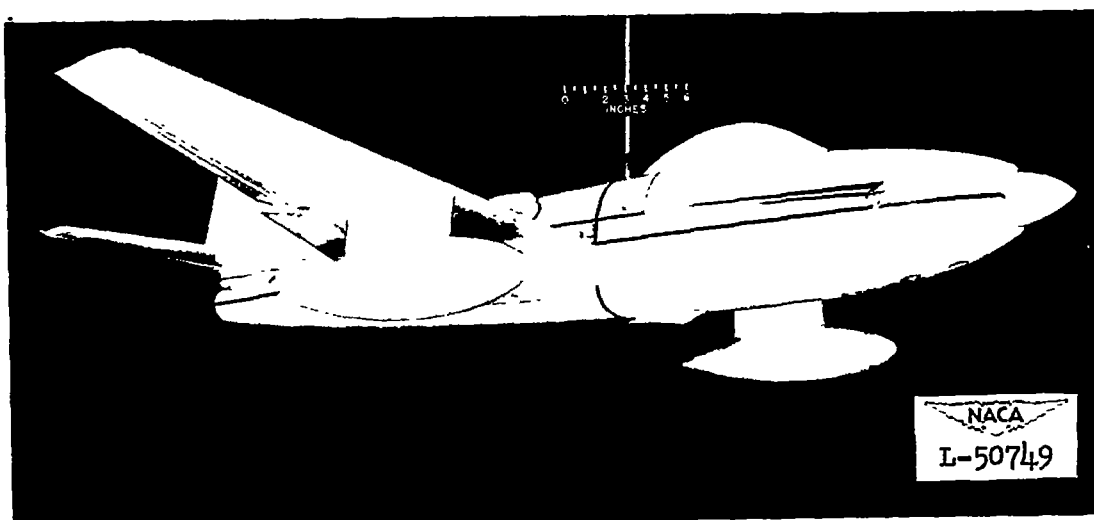


Figure 5.- The  $\frac{1}{10}$ -scale model of a fighter airplane in the clean condition.





Landing condition



External wing fuel tanks installed

Figure 6.- The  $\frac{1}{10}$ -scale model of a fighter airplane in the landing condition and with external wing fuel tanks installed.



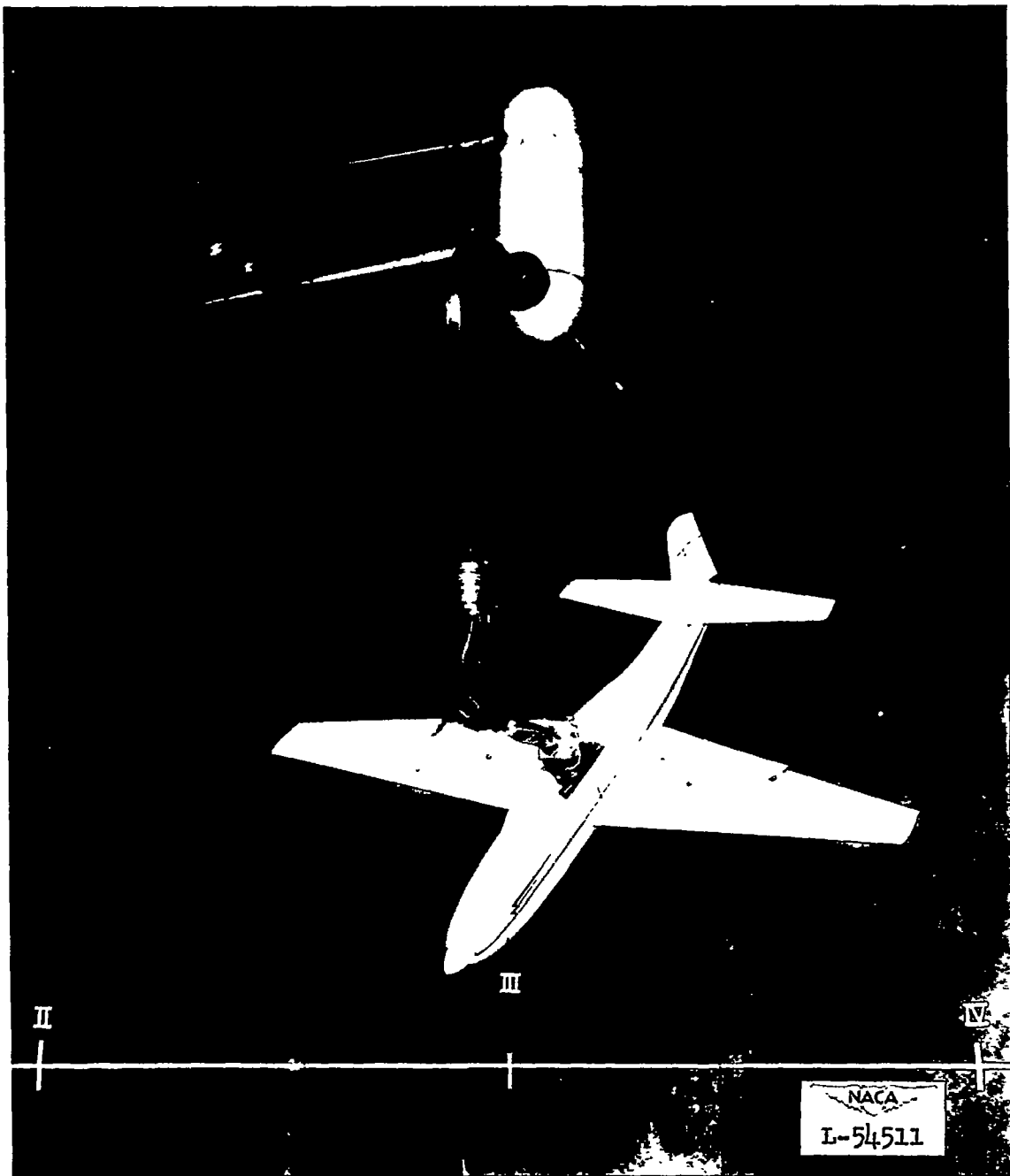
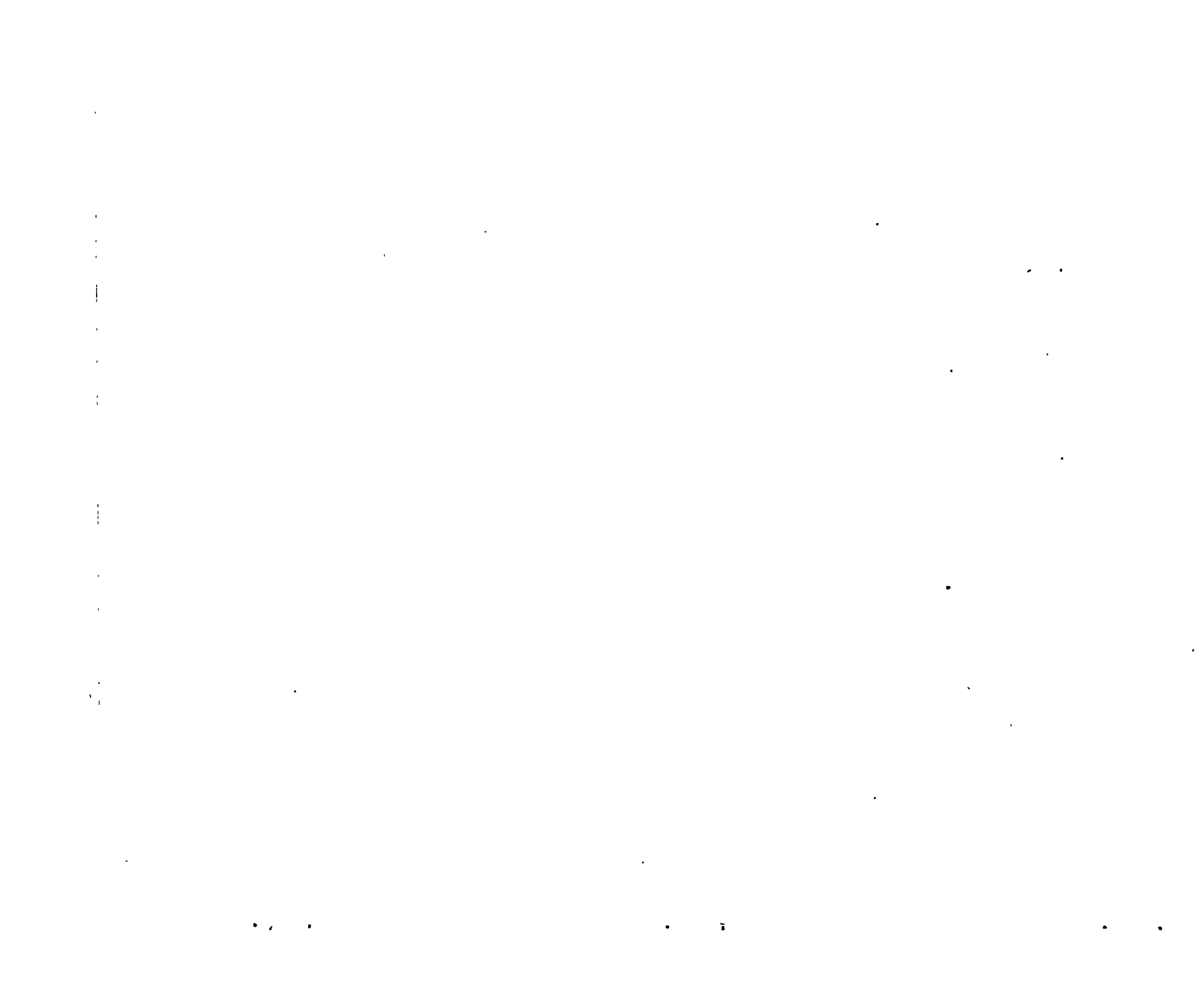


Figure 7.- The  $\frac{1}{10}$ -scale model of a fighter airplane mounted on the rotary balance in the Langley 20-foot free-spinning tunnel.

—



Figure 8.- Photograph of the  $\frac{1}{20}$ -scale model of a fighter airplane spinning in the Langley 20-foot free-spinning tunnel.



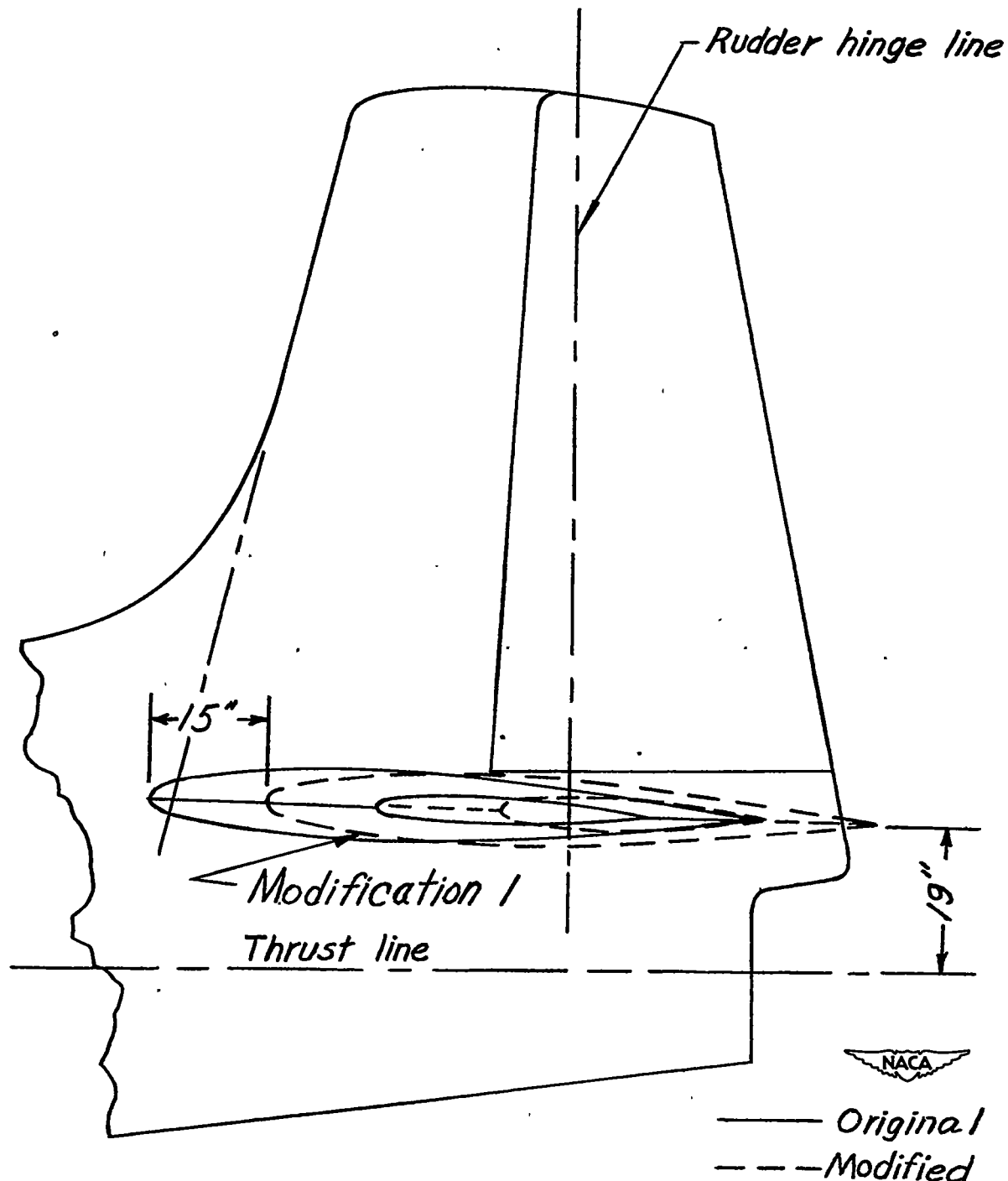


Figure 9.- Original and modified longitudinal positions of horizontal tail tested on the  $\frac{1}{20}$ - scale and  $\frac{1}{10}$ - scale models of a fighter airplane. Dimensions are full-scale.

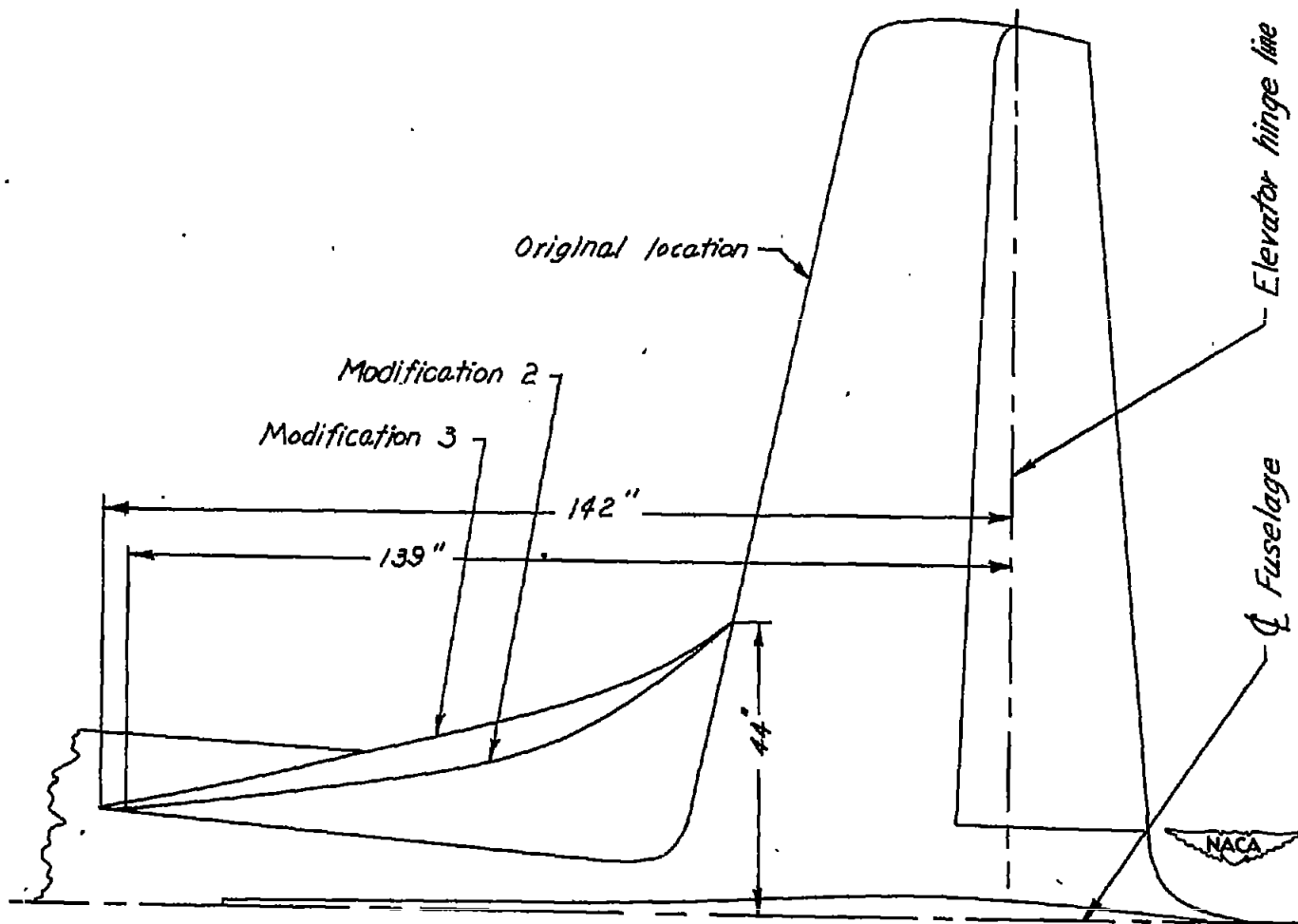


Figure 10.- Original location of the horizontal tail tested and the anti-spin fillets tested on the  $\frac{1}{20}$ -scale and  $\frac{1}{10}$ -scale models of a fighter airplane. Dimensions are full-scale.

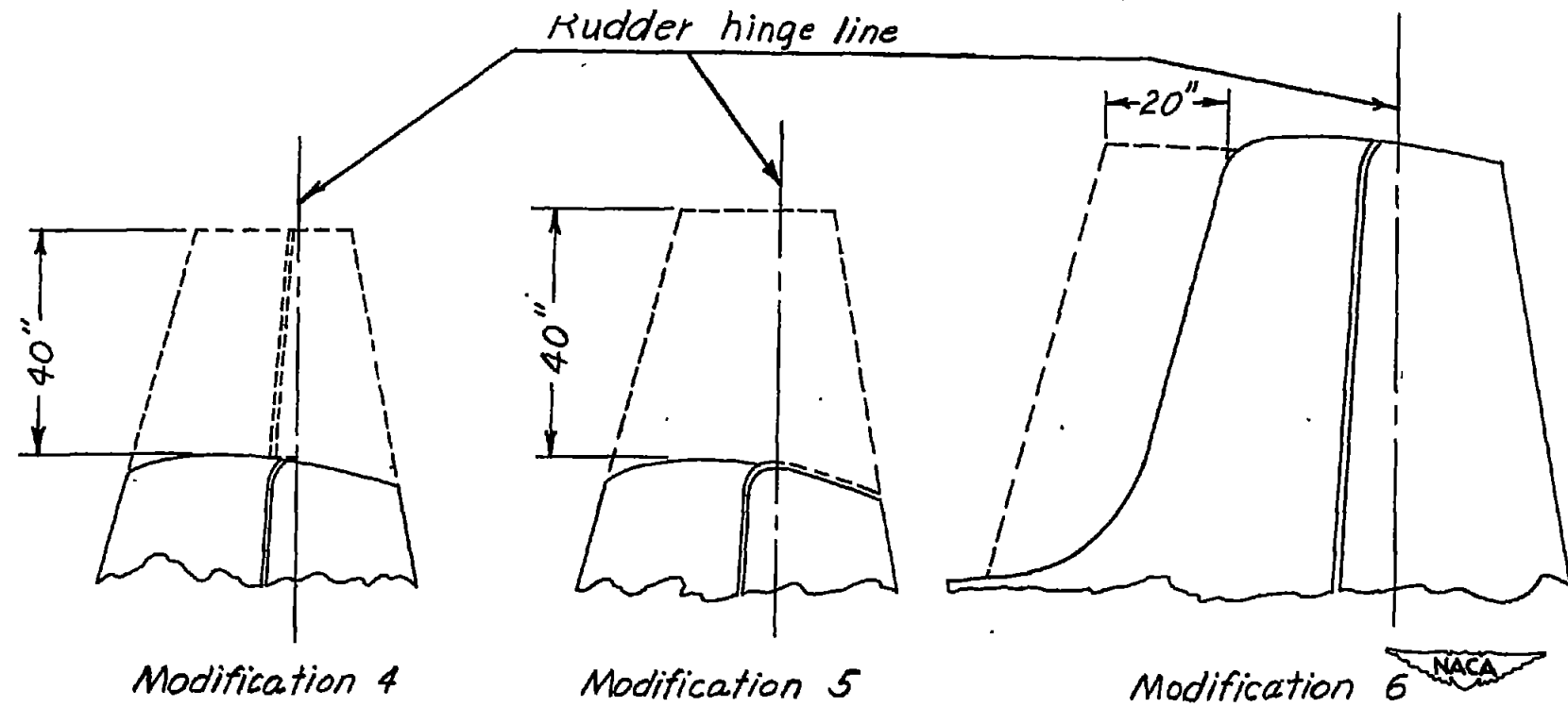


Figure 11.- Modifications to the vertical tail tested on the  $\frac{1}{20}$ -scale  
and  $\frac{1}{10}$ -scale models of a fighter airplane. Dimensions are full-scale.

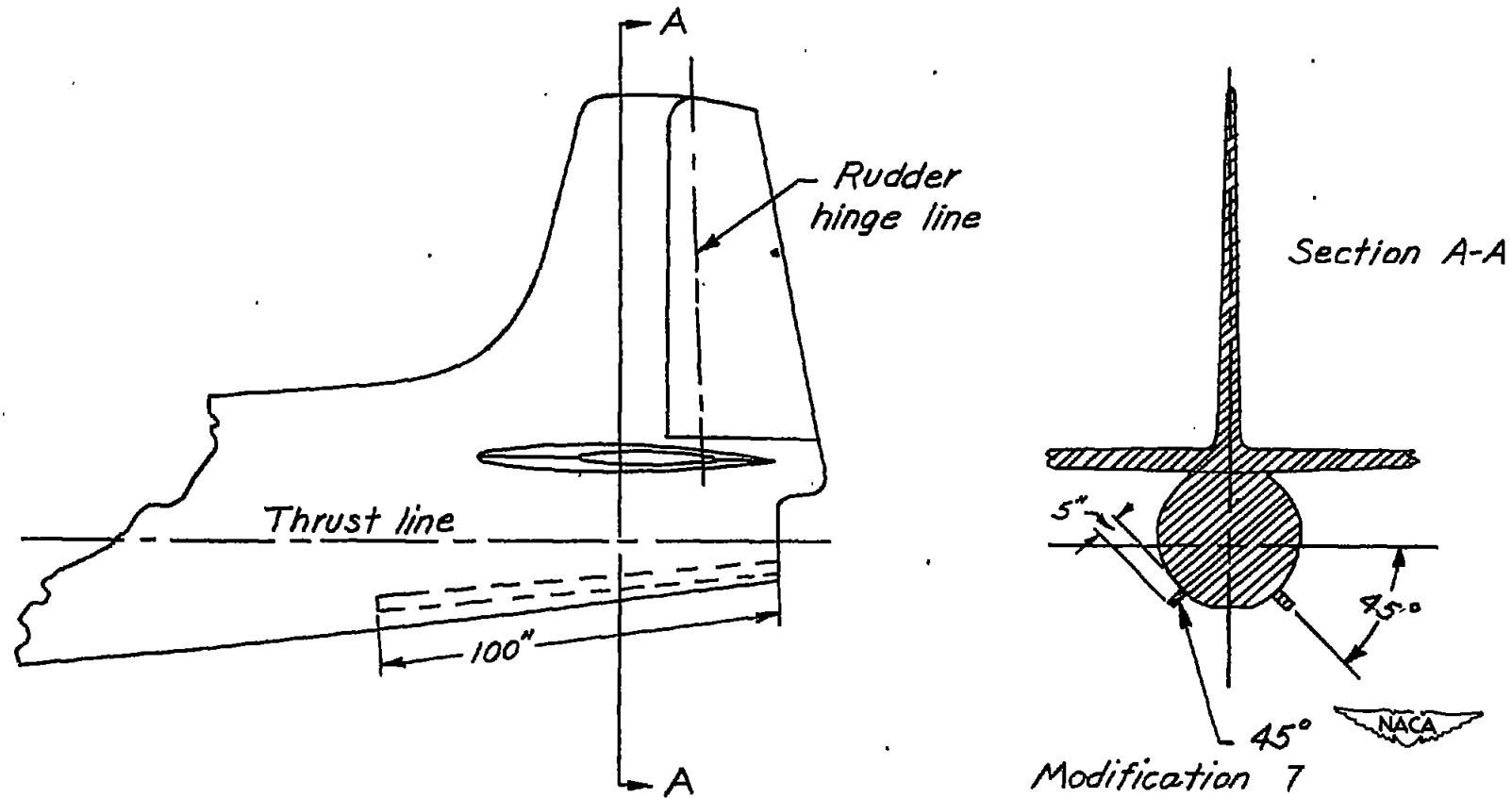


Figure 12.- Ventral fins tested on the  $\frac{1}{20}$ -scale and  $\frac{1}{10}$ -scale models of a fighter airplane. Dimensions are full-scale.

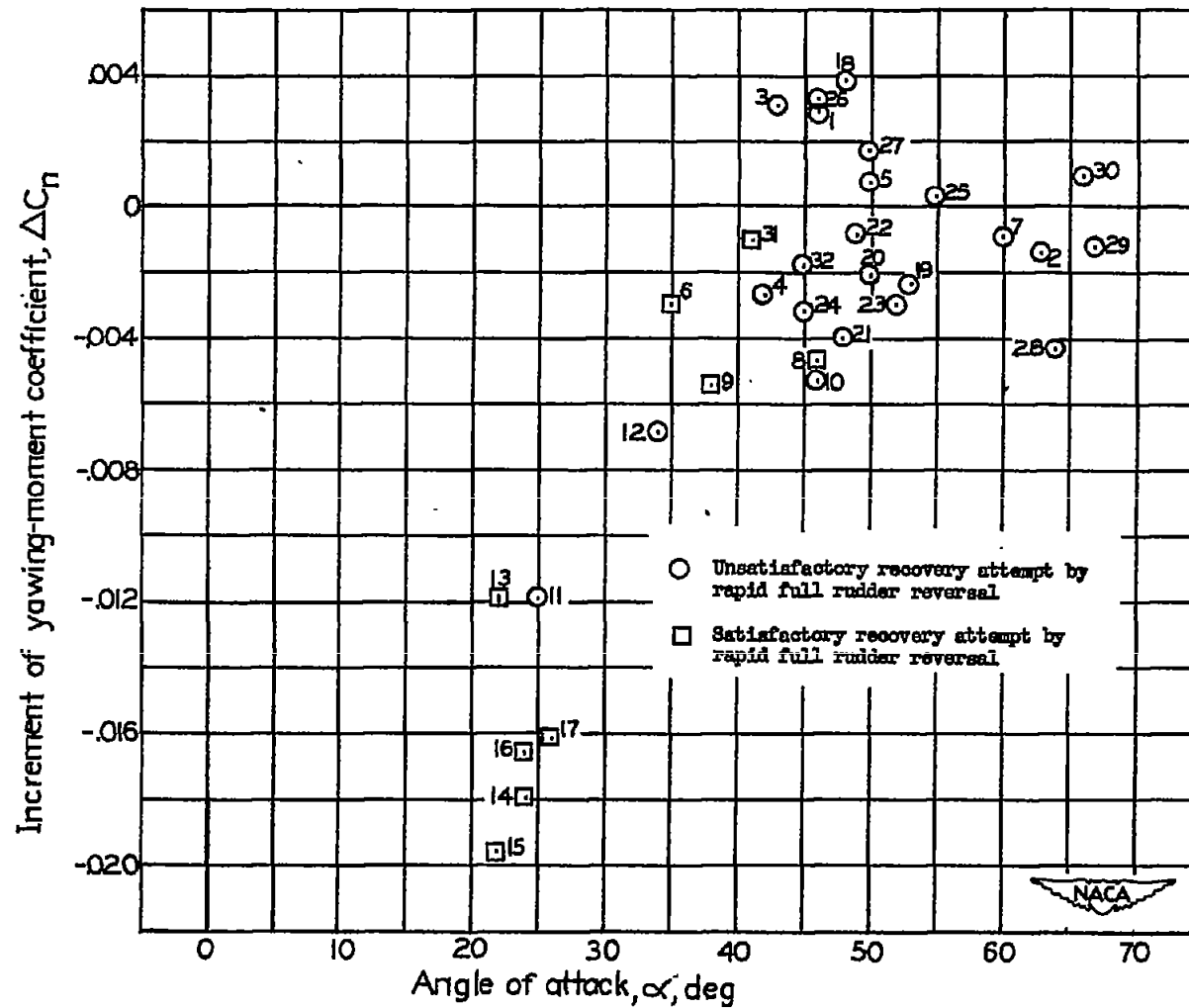


Figure 13.- Variation of the increment of yawing-moment coefficient caused by rudder reversal with angle of attack for spins of a model of a fighter airplane. Numbers refer to test conditions in table III.

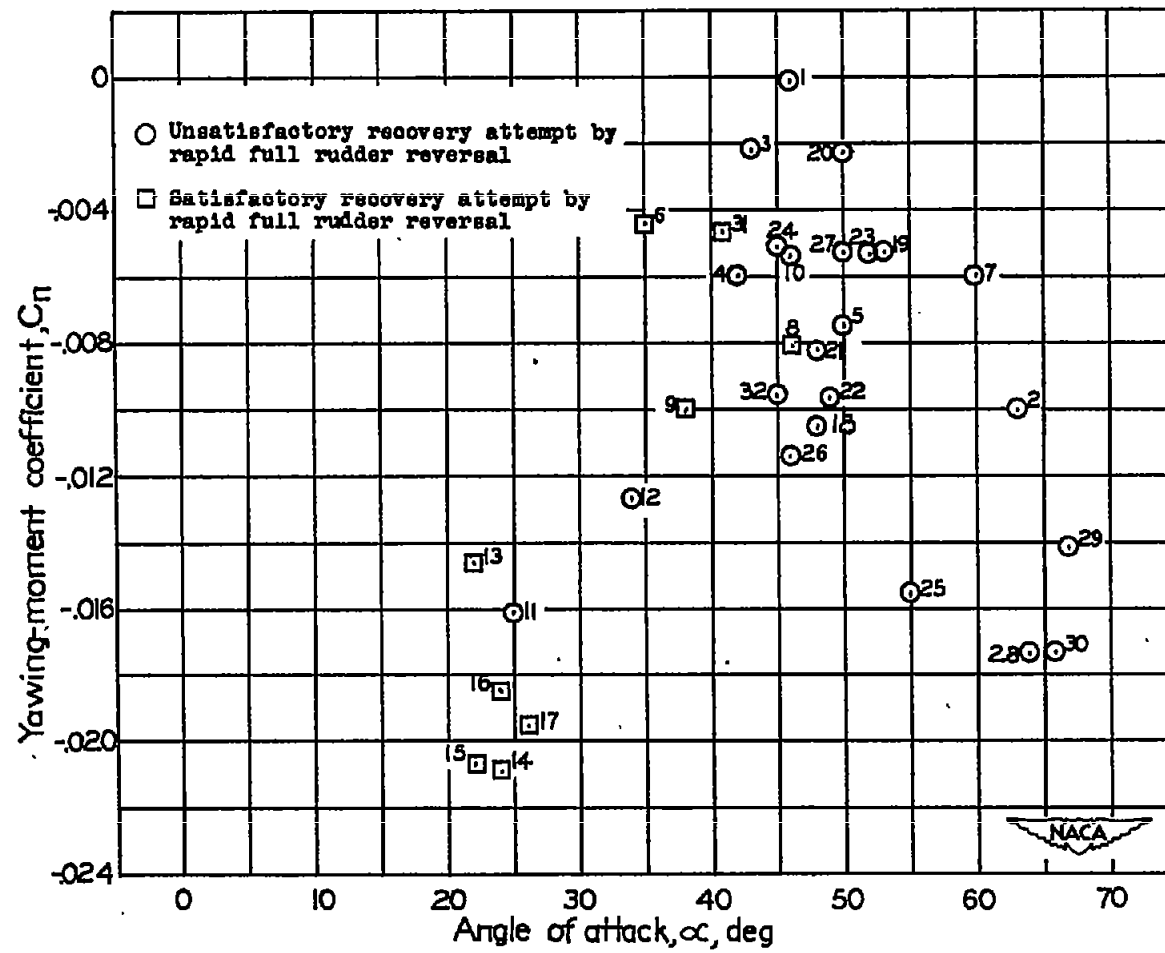


Figure 14.- Variation of yawing-moment coefficient caused by setting the rudder against the spin with angle of attack for spins of a model of a fighter airplane. Numbers refer to test conditions in table III.

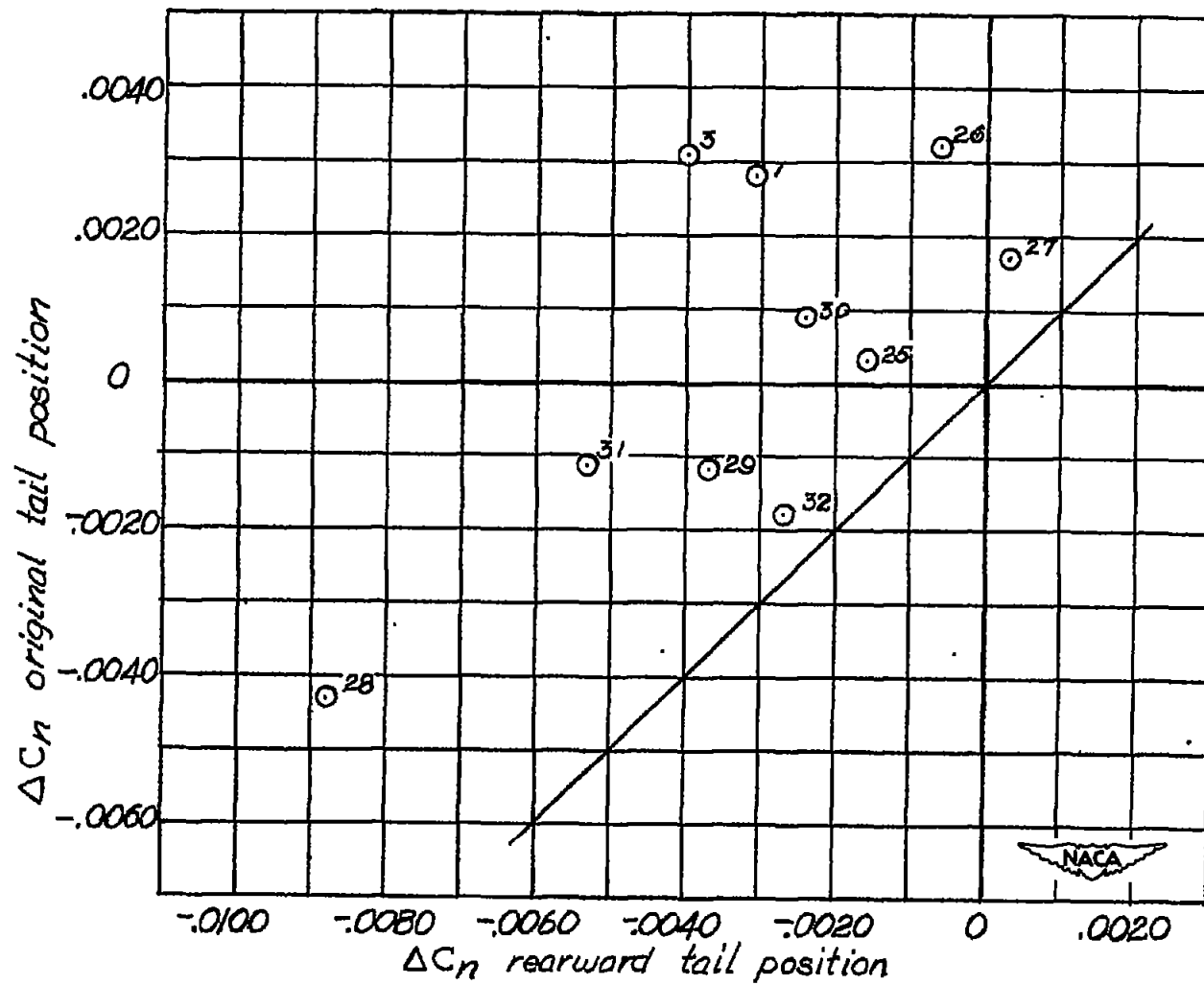


Figure 15.- Effect of horizontal-tail position on the increment of yawing-moment coefficient caused by rudder reversal for spins of a model of a fighter airplane. Numbers refer to test conditions in table III.